AIMS Mathematics, 9(6): 16721–16752.
DOI: 10.3934/math.2024811
Received: 24 March 2024
Revised: 02 May 2024
Accepted: 07 May 2024
Published: 14 May 2024

http://www.aimspress.com/journal/Math

Research article

Analytical study of time-fractional heat, diffusion, and Burger's equations using Aboodh residual power series and transform iterative methodologies

Humaira Yasmin[1,2,*] **and Aljawhara H. Almuqrin**[3]

[1] Department of Basic Sciences, General Administration of Preparatory Year, King Faisal University, P.O. Box 400, Al Ahsa 31982, Saudi Arabia

[2] Department of Mathematics and Statistics, College of Science, King Faisal University, P.O. Box 400, Al Ahsa 31982, Saudi Arabia

[3] Department of Physics, College of Science, Princess Nourah bint Abdulrahman University, P.O. Box 84428, Riyadh 11671, Saudi Arabia

* **Correspondence:** Email: hhassain@kfu.edu.sa.

Abstract: Within the framework of time fractional calculus using the Caputo operator, the Aboodh residual power series method and the Aboodh transform iterative method were implemented to analyze three basic equations in mathematical physics: the heat equation, the diffusion equation, and Burger's equation. We investigated the analytical solutions of these equations using Aboodh techniques, which provide practical and precise methods for solving fractional differential equations. We clarified the behavior and properties of the obtained approximations using the suggested methods through exact mathematical derivations and computational analysis. The obtained approximations were analyzed numerically and graphically to verify their high accuracy and stability against different related parameters. Additionally, we examined the impact of varying the fractional parameter the profiles of all derived approximations. Our results confirm these methods, efficacy in capturing the complicated dynamics of fractional systems. Therefore, they enhance the comprehension and examination of time-fractional equations in many scientific and technical contexts and in modeling different physical problems related to fluid mediums and plasma physics.

Keywords: fractional heat equations; diffusion equations; Burger's equations; Aboodh residual power series method; Aboodh transform iterative method; Caputo operator
Mathematics Subject Classification: 34G20, 35A20, 35A22, 35R11

1. Introduction

Fractional calculus (FC) is a subfield of mathematics that deals with integrals and derivatives of complex or arbitrary orders [1–5], also being named non-Newtonian and extended calculus. L'Hospital questioned the implications of derivative of order 1/2 [6–8]. The answer from Leibniz on September 30, 1695, is recognized as the origin of the non-Newtonian calculus. Fractional calculus is beneficial in many scientific fields, including engineering, physics, signal and fiber optics, chemistry, biology, control theory, viscoelasticity, solid-state and stochastic finance, and economics, to mention a few [9–12]. Although there are numerous fractional definitions of derivatives, not all of them have gained widespread use. The Atangana-Baleanu fractional derivative, Caputo-Fabrizio fractional derivative, conformable operators, Riemann-Liouville (R-L) derivative, and Caputo fractional derivative are the most well-known [13–15]. When describing complex systems with high-order dynamics and sophisticated nonlinear processes, it may be better to use fractional than integer-order derivatives. Two primary characteristics are explain for this. First, fractional derivatives can have any order, not just integral [16–18]. Second, the non-integer order derivative is useful, as it allows the system to retain a long-lasting memory , incorporating information from both the past and the present [19, 20].

In 1885, Adolf Fick described his laws of dispersion. Later, Fick's second law was dubbed the diffusion equation. Diffusion is the system by which atoms or molecules slowly shift from high to low chemical potential areas. Other researchers have extended the classical diffusion and wave equations to describe other physical systems slow diffusion, the classical wave equations, and the diffusion-wave hybrid [21]. Electrochemistry, acoustics, electromagnetic and phase phenomena, filtrations, organic chemistry, bacteriology, cosmology, and system dynamics are among the many areas where the diffusion equation is commonly used [22]. Ficks's second law of dispersion applies the spread of substances in a medium in response to chemical potential gradients. One or more variable's comparative value forms a gradient, which are expressed as measures of one or more variables, primarily independent ones [23]. A variety of factors may contribute to the formation of entropy in engineering systems. As investigated in an influential series of papers by Bejan and colleagues [24], mass transfer, heat transfer, viscous dissipation, thermal coupling, electrical conduction, and chemical reactions are the primary mechanisms by which entropy is produced in thermal systems. The collocation method (CM) [25], diffusion and Tsallis entropy [26], entropy production, symmetric fractional diffusion [27], and many other techniques have been used for the solution of the diffusion equation [28–32].

In 1822, the heat equation was formulated by Joseph Fourier. The relationship between the heat equation and Brownian motion. Particles in suspension in a gas or fluid generate wavelike motion when they collide with the fluid's fast-moving atoms. The transferred particles' dynamic energy is known as heat. When thermal energy is transferred from a warmer object to a cooler one, this causes the atoms in the latter to move faster and collide with its boundaries. This transfers some of this energy to the system's atoms, causing them to move faster [33]. In classical physics, the wave equation describes waves in terms of fluid dynamics, mechanical waves, and the electromagnetic wave equation, which is a significant second-order linear PDE in acoustics, electromagnetics, and fluid dynamics. Light, sound, gravity, and matter (including the Klein-Gordon equation in relativistic quantum physics) are all examples of phenomena governed by this equation. Alembert and Euler discovered the wave equation

in one and three dimensions. Numerous mathematicians have contributed to solutions heat and wave equations, employing methods such as the optimal homotopy asymptotic method (OHAM) [34], the modified Adomian decomposition method (MADM) [35], and many others [36–39].

The Galerkin method was used by R. Mittal and P. Singhal [40] to find numerical solutions to Burgers' equation. In light of this, scientists have worked very hard to solve the fractional Burgers' equation analytically and/or numerically. A. Esen and O. Tasbozan [41] provided a numerical solution of the time-fractional Burgers' equation using cubic B-spline finite elements as one example. A. Esen et al. [42] used that homotopy analysis method (HAM) to solve the time-fractional Burgers' equation analytically. Additionally, E. Abdel Salam et al. [43] solved the space-time fractional Burgers' equation using the fractional Riccati expansion technique. M. Inc. solved the space-time-fractional Burgers' equations using a variational iteration approach [44].

Residual power series method (RPSM) was created in 2013 by Omar Abu Arqub [45]. It was formed by combining the Taylor series with the residual error function. For DEs, the solution is provided by an infinite convergence series [46]. Novel RPSM algorithms that seek to provide efficient and precise approximation solutions have been developed in response to a variety of DEs, such as Boussinesq DEs, fuzzy DEs, KdV-Burger's equation, and many more [47–52].

A novel approach for solving fractional-order differential equations (FDEs) was developed by combining two efficient techniques. Namely, the Sumudu transform has been combined with the Shehu transformation and the Adomian decomposition method [53], and the Laplace transform has been combined with RPSM [54–56], the natural transform [57], and the homotopy perturbation approach [58]. See [59, 60] for more information on the combination of these methods

The fundamental idea of the new approach is to convert the original problem into an Aboodh transform space, identify many solutions to the transformed version of the equation, and then use the inverse Aboodh transform to solve the original equation. With power series expansion, the new approach may be utilized to solve linear and nonlinear PDEs without discretization, linearization, or perturbation. This method does not depend on matching coefficients of related terms or recursion relations, which sets it apart from the traditional power series methodology. In contrast to the RPSM, the proposed limit-based approach reveals series coefficients instead of fractional derivatives.

Two straightforward methods can be used for solving fractional differential equations, named ATIM and Aboodh residual power series method (ARPSM), as mentioned in [59, 60]. Both methods do not only return a numerical solution free from any discretization or linearization of PDEs but also, at the same time, instantly and explicitly display a symbolic representation of the result. For example, these techniques were used to analyze the fractional Hirota-Satsuma coupled Korteweg-de Vries (KdV) problem and derive some highly accurate approximations. The results were effective, accurate, and stable [61]. These methods also succeeded in analyzing some of the most widespread evolution equations in plasma physics and fluid physics, called the Berger-type equations. Some analytical approximations for the damp Burger equation and some related equations were derived, and the accuracy of the derived approximations was tested in a number of different ways to verify the effectiveness of the suggested methods [62]. Moreover, these approaches were used for solving more complicated and strong nonlinear fractional physical equations, as illustrated in [63]. This study introduces ARPSM and ATIM to solve the time-fractional equations of heat, diffusion, and Burger's equations. Compared with other numerical techniques, these approaches provide numerical solutions that are more exact and accurate. The numerical results are also subjected to comparison analysis.

The results of the proposed methodologies show good agreement with each other, indicating their effectiveness and dependability, with extra graphical significance for various values of fractional-order derivatives. As a result, the techniques are precise, simple to use, impervious to computational error cycles, and time-efficient. Other researchers will be able to solve various partial differential equations with ease because of the foundation this study provides.

2. Definitions

Definition 2.1. *[64] If $\omega(\mu,\tau)$ is an exponentially ordered piecewise continuous function, then the Aboodh transform (AT) for $\sigma \geq 0$ can be defined by*

$$A[\omega(\mu,\tau)] = \Psi(\mu,\xi) = \frac{1}{\xi}\int_0^\infty \omega(\mu,\tau)e^{-\tau\xi}d\tau, \quad r_1 \leq \xi \leq r_2.$$

The following is one specific definition of the Aboodh inverse transform (AIT):

$$A^{-1}[\Psi(\mu,\xi)] = \omega(\mu,\tau) = \frac{1}{2\pi i}\int_{u-i\infty}^{u+i\infty} \Psi(\mu,\tau)\xi e^{\tau\xi}d\tau,$$

where $\mu = (\mu_1,\mu_2,\cdots,\mu_p) \in \mathbb{R}$ and $p \in \mathbb{N}$.

Lemma 2.1. *[65,66] Two piecewise continuous functions that are exponentially ordered are assumed to exist, $\omega_1(\mu,\tau)$ and $\omega_2(\mu,\tau)$ on $[0,\infty[$. Let $A[\omega_1(\mu,\tau)] = \Psi_1(\mu,\tau), A[\omega_2(\mu,\tau)] = \Psi_2(\mu,\tau)$ and χ_1,χ_2 are constants. For that reason, the following features are true:*

(1) $A[\chi_1\omega_1(\mu,\tau) + \chi_2\omega_2(\mu,\tau)] = \chi_1\Psi_1(\mu,\xi) + \chi_2\Psi_2(\mu,\tau)$,
(2) $A^{-1}[\chi_1\Psi_1(\mu,\tau) + \chi_2\Psi_2(\mu,\tau)] = \chi_1\omega_1(\mu,\xi) + \chi_2\omega_2(\mu,\tau)$,
(3) $A[J_\tau^p\omega(\mu,\tau)] = \frac{\Psi(\mu,\xi)}{\xi^p}$,
(4) $A[D_\tau^p\omega(\mu,\tau)] = \xi^p\Psi(\mu,\xi) - \sum_{K=0}^{r-1}\frac{\omega^K(\mu,0)}{\xi^{K-p+2}}, r-1 < p \leq r,\ r \in \mathbb{N}$.

Definition 2.2. *[67] The fractional derivative of the function $\omega(\mu,\tau)$ is defined by the Caputo operator as follows, with respect to order p:*

$$D_\tau^p\omega(\mu,\tau) = J_\tau^{m-p}\omega^{(m)}(\mu,\tau),\ r \geq 0,\ m-1 < p \leq m,$$

where $\mu = (\mu_1,\mu_2,\cdots,\mu_p) \in \mathbb{R}^p$ and $m, p \in R$, J_τ^{m-p} is the R-L integral of $\omega(\mu,\tau)$.

Definition 2.3. *[68] The power series form reads*

$$\sum_{r=0}^{\infty}\hbar_r(\mu)(\tau-\tau_0)^{rp} = \hbar_0(\tau-\tau_0)^0 + \hbar_1(\tau-\tau_0)^p + \hbar_2(\tau-\tau_0)^{2p} + \cdots,$$

where $\mu = (\mu_1,\mu_2,\cdots,\mu_p) \in \mathbb{R}^p$ and $p \in \mathbb{N}$. The variable τ and the series coefficients in a multiple fractional power series (MFPS) are $\hbar_r(\mu)'s$, and the series is about τ_0.

Lemma 2.2. *Let $\omega(\mu,\tau)$ be the exponential order function. The AT is defined as follows: $A[\omega(\mu,\tau)] = \Psi(\mu,\xi)$. Hence,*

$$A[D_\tau^{rp}\omega(\mu,\tau)] = \xi^{rp}\Psi(\mu,\xi) - \sum_{j=0}^{r-1}\xi^{p(r-j)-2}D_\tau^{jp}\omega(\mu,0), 0 < p \leq 1, \tag{2.1}$$

where $\mu = (\mu_1,\mu_2,\cdots,\mu_p) \in \mathbb{R}^p$ and $p \in \mathbb{N}$ and $D_\tau^{rp} = D_\tau^pD_\tau^p\cdots D_\tau^p(r-times)$.

Proof. We may prove Eq (2.1) via induction. Using $r = 1$ in Eq (2.1) yields the following results:

$$A[D_{\tau}^{2p}\omega(\mu,\tau)] = \xi^{2p}\Psi(\mu,\xi) - \xi^{2p-2}\omega(\mu,0) - \xi^{p-2}D_{\tau}^{p}\omega(\mu,0).$$

Lemma 2.1, states that Eq (2.1) is true for $r = 1$. For $r = 2$, the result is given by Eq (2.1).

$$A[D_{r}^{2p}\omega(\mu,\tau)] = \xi^{2p}\Psi(\mu,\xi) - \xi^{2p-2}\omega(\mu,0) - \xi^{p-2}D_{\tau}^{p}\omega(\mu,0). \tag{2.2}$$

The left-hand side (L.H.S) of Eq (2.2) allows us to get

$$L.H.S = A[D_{\tau}^{2p}\omega(\mu,\tau)]. \tag{2.3}$$

The expressions of Eq (2.3) read

$$L.H.S = A[D_{\tau}^{p}(D_{\tau}^{p}\omega(\mu,\tau))]. \tag{2.4}$$

Let

$$z(\mu,\tau) = D_{\tau}^{p}\omega(\mu,\tau). \tag{2.5}$$

Thus, Eq (2.4) becomes

$$L.H.S = A[D_{\tau}^{p}z(\mu,\tau)]. \tag{2.6}$$

Equation (2.6) is changed due to the utilization of the Caputo derivative

$$L.H.S = A[J^{1-p}z^{'}(\mu,\tau)]. \tag{2.7}$$

The R-L integral for AT, which is given in Eq (2.7), may be used to get

$$L.H.S = \frac{A[z^{'}(\mu,\tau)]}{\xi^{1-p}}. \tag{2.8}$$

Using the AT's derivative property, then Eq (2.8) may be changed into the following format:

$$L.H.S = \xi^{p}Z(\mu,\xi) - \frac{z(\mu,0)}{\xi^{2-p}}. \tag{2.9}$$

From Eq (2.5), we obtain

$$Z(\mu,\xi) = \xi^{p}\Psi(\mu,\xi) - \frac{\omega(\mu,0)}{\xi^{2-p}},$$

where $A[z(\mu,\tau)] = Z(\mu,\xi)$. Therefore, Eq (2.9) is transformed into the following form

$$L.H.S = \xi^{2p}\Psi(\mu,\xi) - \frac{\omega(\mu,0)}{\xi^{2-2p}} - \frac{D_{\tau}^{p}\omega(\mu,0)}{\xi^{2-p}}, \tag{2.10}$$

when $r = K$. Eqs (2.1) and (2.10) are compatible. Assuming that for $r = K$, the Eq (2.1) the hold true, let us proceed, we put $r = K$ in Eq (2.1):

$$A[D_{\tau}^{Kp}\omega(\mu,\tau)] = \xi^{Kp}\Psi(\mu,\xi) - \sum_{j=0}^{K-1}\xi^{p(K-j)-2}D_{\tau}^{jp}D_{\tau}^{jp}\omega(\mu,0),\ 0 < p \leq 1. \tag{2.11}$$

The next step is to illustrate Eq (2.1) for the value of $r = K + 1$. Using Eq (2.1), we can write

$$A[D_{\tau}^{(K+1)p}\omega(\mu,\tau)] = \xi^{(K+1)p}\Psi(\mu,\xi) - \sum_{j=0}^{K}\xi^{p((K+1)-j)-2}D_{\tau}^{jp}\omega(\mu,0). \tag{2.12}$$

After examining the left-hand side of Eq (2.12), we get

$$L.H.S = A[D_{\tau}^{Kp}(D_{\tau}^{Kp})]. \tag{2.13}$$

Let

$$D_{\tau}^{Kp} = g(\mu,\tau).$$

By Eq (2.13), we drive

$$L.H.S = A[D_{\tau}^{p}g(\mu,\tau)]. \tag{2.14}$$

Applying the Caputo derivative and R-L integral to Eq (2.14) yields the following result

$$L.H.S = \xi^{p}A[D_{\tau}^{Kp}\omega(\mu,\tau)] - \frac{g(\mu,0)}{\xi^{2-p}}. \tag{2.15}$$

Equation (2.11) is used to get

$$L.H.S = \xi^{rp}\Psi(\mu,\xi) - \sum_{j=0}^{r-1}\xi^{p(r-j)-2}D_{\tau}^{jp}\omega(\mu,0). \tag{2.16}$$

Moreover, the following outcome is obtained using Eq (2.16):

$$L.H.S = A[D_{\tau}^{rp}\omega(\mu,0)].$$

For $r = K+1$, the Eq (2.1) so holds. Therefore, Eq (2.1) is true for all positive integers via mathematical induction. □

A novel interpretation of multiple fractional Taylor's series (MFTS) is given in the following lemma. This formula will be useful for the ARPSM (explained below).

Lemma 2.3. *Assume that $\omega(\mu,\tau)$ is the exponential order function. The equation $A[\omega(\mu,\tau)] = \Psi(\mu,\xi)$ is the AT of $\omega(\mu,\tau)$. The MFTS notation for AT reads*

$$\Psi(\mu,\xi) = \sum_{r=0}^{\infty}\frac{\hbar_r(\mu)}{\xi^{rp+2}}, \xi > 0, \tag{2.17}$$

where, $\mu = (s_1,\mu_2,\cdots,\mu_p) \in \mathbb{R}^p,\ p \in \mathbb{N}$.

Proof. Let us investigate Taylor's series' fractional order expression:

$$\omega(\mu,\tau) = \hbar_0(\mu) + \hbar_1(\mu)\frac{\tau^p}{\Gamma[p+1]} + +\hbar_2(\mu)\frac{\tau^{2p}}{\Gamma[2p+1]} + \cdots \tag{2.18}$$

The following equation represents the equality that is achieved when Eq (2.18) is processed using the AT:

$$A\left[\omega(\mu,\tau)\right] = A\left[\hbar_0(\mu)\right] + A\left[\hbar_1(\mu)\frac{\tau^p}{\Gamma[p+1]}\right] + A\left[\hbar_1(\mu)\frac{\tau^{2p}}{\Gamma[2p+1]}\right] + \cdots$$

The AT's features allow for this to be accomplished.

$$A\left[\omega(\mu,\tau)\right] = \hbar_0(\mu)\frac{1}{\xi^2} + \hbar_1(\mu)\frac{\Gamma[p+1]}{\Gamma[p+1]}\frac{1}{\xi^{p+2}} + \hbar_2(\mu)\frac{\Gamma[2p+1]}{\Gamma[2p+1]}\frac{1}{\xi^{2p+2}}\cdots$$

As a result, (2.17) is obtained, which is a special version of Taylor's s eries in the AT. □

Lemma 2.4. *To illustrate the MFPS in its new form, as stated in Taylor's series* (2.17)*, let* $A[\omega(\mu,\tau)] = \Psi(\mu,\xi)$.

$$\hbar_0(\mu) = \lim_{\xi\to\infty}\xi^2\Psi(\mu,\xi) = \omega(\mu,0). \tag{2.19}$$

Proof. The novel formulation of Taylor's series allows us to infer the preceding:

$$\hbar_0(\mu) = \xi^2\Psi(\mu,\xi) - \frac{\hbar_1(\mu)}{\xi^p} - \frac{\hbar_2(\mu)}{\xi^{2p}} - \cdots \tag{2.20}$$

The necessary solution may be obtained by putting $\lim_{\xi\to\infty}$ into Eq (2.19) and doing a quick computation, as shown in Eq (2.20). □

Theorem 2.1. *This is the MFPS notation for the function* $A[\omega(\mu,\tau)] = \Psi(\mu,\xi)$.

$$\Psi(\mu,\xi) = \sum_0^\infty \frac{\hbar_r(\mu)}{\xi^{rp+2}},\ \xi > 0,$$

where $\mu = (\mu_1,\mu_2,\cdots,\mu_p) \in \mathbb{R}^p$ *and* $p \in \mathbb{N}$. *Then we have*

$$\hbar_r(\mu) = D_r^{rp}\omega(\mu,0),$$

where $D_\tau^{rp} = D_\tau^p.D_\tau^p.\cdots.D_\tau^p(r-times)$.

Proof. The new Taylor's series is as follows:

$$\hbar_1(\mu) = \xi^{p+2}\Psi(\mu,\xi) - \xi^p\hbar_0(\mu) - \frac{\hbar_2(\mu)}{\xi^p} - \frac{\hbar_3(\mu)}{\xi^{2p}} - \cdots \tag{2.21}$$

$\lim_{\xi\to\infty}$, is applied to Eq (2.21), we get

$$\hbar_1(\mu) = \lim_{\xi\to\infty}(\xi^{p+2}\Psi(\mu,\xi) - \xi^p\hbar_0(\mu)) - \lim_{\xi\to\infty}\frac{\hbar_2(\mu)}{\xi^p} - \lim_{\xi\to\infty}\frac{\hbar_3(\mu)}{\xi^{2p}} - \cdots$$

We get the following equality by taking the limit:

$$\hbar_1(\mu) = \lim_{\xi\to\infty}(\xi^{p+2}\Psi(\mu,\xi) - \xi^p\hbar_0(\mu)). \tag{2.22}$$

The result of applying Lemma 2.2 into Eq (2.22) reads

$$\hbar_1(\mu) = \lim_{\xi\to\infty}(\xi^2 A[D_\tau^p\omega(\mu,\tau)](\xi)). \tag{2.23}$$

Moreover, it is transformed into by using Lemma 2.3 to the Eq (2.23)

$$\hbar_1(\mu) = D_\tau^p \omega(\mu, 0).$$

Again, assuming limit $\xi \to \infty$ and using the new form of Taylor's series, we get

$$\hbar_2(\mu) = \xi^{2p+2}\Psi(\mu, \xi) - \xi^{2p}\hbar_0(\mu) - \xi^p \hbar_1(\mu) - \frac{\hbar_3(\mu)}{\xi^p} - \cdots$$

The outcome is given by Lemma 2.3

$$\hbar_2(\mu) = \lim_{\xi\to\infty} \xi^2(\xi^{2p}\Psi(\mu, \xi) - \xi^{2p-2}\hbar_0(\mu) - \xi^{p-2}\hbar_1(\mu)). \tag{2.24}$$

Equation (2.24) is transformed into the following form using Lemmas 2.2 and 2.4

$$\hbar_2(\mu) = D_\tau^{2p} \omega(\mu, 0).$$

The subsequent results are acquired through the application of the identical procedure to the new Taylor's series:

$$\hbar_3(\mu) = \lim_{\xi\to\infty} \xi^2(A[D_\tau^{2p}\omega(\mu, p)](\xi)).$$

Lemma 2.4 is employed to figure out the final equation.

$$\hbar_3(\mu) = D_\tau^{3p} \omega(\mu, 0).$$

In general,

$$\hbar_r(\mu) = D_\tau^{rp} \omega(\mu, 0).$$

Consequently, the proof is concluded. □

The laws regulating the convergence of Taylor's series in its modified form are delineated and validated in the following theorem.

Theorem 2.2. *The new form of the formula for multiple fractional Taylor's, as presented in Lemma 2.3, is as follows:* $A[\omega(\mu, \tau)] = \Psi(\mu, \xi)$. *When* $|\xi^a A[D_\tau^{(K+1)p}\omega(\mu, \tau)]| \le T$, *for all* $0 < \xi \le s$ *and* $0 < p \le 1$, *the residual* $R_K(\mu, \xi)$ *of the newly developed MFTS satisfies the inequality:*

$$|R_K(\mu, \xi)| \le \frac{T}{\xi^{(K+1)p}},\ 0 < \xi \le s.$$

Proof. Assume $A[D_\tau^{rp}\omega(\mu, \tau)](\xi)$ is defined on $0 < \xi \le s$ for $r = 0, 1, 2, \cdots, K + 1$. Proceed with the assumption that $|\xi^2 A[D_{\tau^{K+1}}\omega(\mu, tau)]| \le T,\ on\ 0 < \xi \le s$. The following relationship utilizing the new Taylor's series:

$$R_K(\mu, \xi) = \Psi(\mu, \xi) - \sum_{r=0}^{K} \frac{\hbar_r(\mu)}{\xi^{rp+2}}. \tag{2.25}$$

Equation (2.25) is transformed into the following form using Theorem 2.1

$$R_K(\mu, \xi) = \Psi(\mu, \xi) - \sum_{r=0}^{K} \frac{D_\tau^{rp}\omega(\mu, 0)}{\xi^{rp+2}}. \tag{2.26}$$

To solve Eq (2.26), simply multiply both sides by $\xi^{(K+1)a+2}$, which leads to

$$\xi^{(K+1)p+2}R_K(\mu,\xi) = \xi^2(\xi^{(K+1)p}\Psi(\mu,\xi) - \sum_{r=0}^{K}\xi^{(K+1-r)p-2}D_\tau^{rp}\omega(\mu,0)). \tag{2.27}$$

Applying Lemma 2.2 to Eq (2.27) produces the following outcome:

$$\xi^{(K+1)p+2}R_K(\mu,\xi) = \xi^2 A[D_\tau^{(K+1)p}\omega(\mu,\tau)]. \tag{2.28}$$

Taking absolute of Eq (2.28) yields

$$|\xi^{(K+1)p+2}R_K(\mu,\xi)| = |\xi^2 A[D_\tau^{(K+1)p}\omega(\mu,\tau)]|. \tag{2.29}$$

The outcome resulting from the implementation of the conditions outlined in Eq (2.29) is as follows:

$$\frac{-T}{\xi^{(K+1)p+2}} \leq R_K(\mu,\xi) \leq \frac{T}{\xi^{(K+1)p+2}}. \tag{2.30}$$

The required result is derived from Eq (2.30)

$$|R_K(\mu,\xi)| \leq \frac{T}{\xi^{(K+1)p+2}}.$$

Thus, an innovative series convergence condition is established. □

3. Methodologies

3.1. The ARPSM to solve time-fractional PDEs

Our overall model solution was constructed using an ARPSM set of rules, which is elaborated in this section.

Step 1. As the general equation is simplified, we obtain

$$D_\tau^{qp}\omega(\mu,\tau) + \vartheta(\mu)N(\omega) - \delta(\mu,\omega) = 0. \tag{3.1}$$

Step 2. Equation (3.1) is subjected to the AT on both sides in order to obtain:

$$A[D_\tau^{qp}\omega(\mu,\tau) + \vartheta(\mu)N(\omega) - \delta(\mu,\omega)] = 0. \tag{3.2}$$

By employing Lemma 2.2, Eq (3.2) can be transformed into the following form

$$\Psi(\mu,s) = \sum_{j=0}^{q-1}\frac{D_\tau^j\omega(\mu,0)}{s^{qp+2}} - \frac{\vartheta(\mu)Y(s)}{s^{qp}} + \frac{F(\mu,s)}{s^{qp}}, \tag{3.3}$$

where $A[\delta(\mu,\omega)] = F(\mu,s), A[N(\omega)] = Y(s)$.

Step 3. The solution to Eq (3.3) is expressed in the following form:

$$\Psi(\mu,s) = \sum_{r=0}^{\infty}\frac{\hbar_r(\mu)}{s^{rp+2}},\ s > 0.$$

Step 4. The necessary procedures are as follows:

$$\hbar_0(\mu) = \lim_{s\to\infty} s^2\Psi(\mu, s) = \omega(\mu, 0).$$

The outcome is as follows when Theorem 2.2 is applied

$$\hbar_1(\mu) = D_\tau^p \omega(\mu, 0),$$

$$\hbar_2(\mu) = D_\tau^{2p} \omega(\mu, 0),$$

$$\vdots$$

$$\hbar_w(\mu) = D_\tau^{wp} \omega(\mu, 0).$$

Step 5. The formula to determine the $\Psi(\mu, s)$ series after the K^{th} truncation is as follows:

$$\Psi_K(\mu, s) = \sum_{r=0}^{K} \frac{\hbar_r(\mu)}{s^{rp+2}},\ s > 0,$$

$$\Psi_K(\mu, s) = \frac{\hbar_0(\mu)}{s^2} + \frac{\hbar_1(\mu)}{s^{p+2}} + \cdots + \frac{\hbar_w(\mu)}{s^{wp+2}} + \sum_{r=w+1}^{K} \frac{\hbar_r(\mu)}{s^{rp+2}}.$$

Step 6. For the following results, it is necessary to consider the Aboodh residual function (ARF) from Eq (3.3) and the *Kth*-truncated ARF independently:

$$ARes(\mu, s) = \Psi(\mu, s) - \sum_{j=0}^{q-1} \frac{D_\tau^j \omega(\mu, 0)}{s^{jp+2}} + \frac{\vartheta(\mu)Y(s)}{s^{jp}} - \frac{F(\mu, s)}{s^{jp}},$$

and

$$ARes_K(\mu, s) = \Psi_K(\mu, s) - \sum_{j=0}^{q-1} \frac{D_\tau^j \omega(\mu, 0)}{s^{jp+2}} + \frac{\vartheta(\mu)Y(s)}{s^{jp}} - \frac{F(\mu, s)}{s^{jp}}. \tag{3.4}$$

Step 7. Equation (3.4) should be modified by placing $\Psi_K(\mu, s)$ rather than its expansion form

$$\begin{aligned} ARes_K(\mu, s) = &\Big(\frac{\hbar_0(\mu)}{s^2} + \frac{\hbar_1(\mu)}{s^{p+2}} + \cdots + \frac{\hbar_w(\mu)}{s^{wp+2}} + \sum_{r=w+1}^{K} \frac{\hbar_r(\mu)}{s^{rp+2}}\Big) \\ &- \sum_{j=0}^{q-1} \frac{D_\tau^j \omega(\mu, 0)}{s^{jp+2}} + \frac{\vartheta(\mu)Y(s)}{s^{jp}} - \frac{F(\mu, s)}{s^{jp}}. \end{aligned} \tag{3.5}$$

Step 8. To determine the solution to Eq (3.5), multiply each side by s^{Kp+2}

$$\begin{aligned} s^{Kp+2}ARes_K(\mu, s) = s^{Kp+2}\Big(&\frac{\hbar_0(\mu)}{s^2} + \frac{\hbar_1(\mu)}{s^{p+2}} + \cdots + \frac{\hbar_w(\mu)}{s^{wp+2}} + \sum_{r=w+1}^{K} \frac{\hbar_r(\mu)}{s^{rp+2}} \\ &- \sum_{j=0}^{q-1} \frac{D_\tau^j \omega(\mu, 0)}{s^{jp+2}} + \frac{\vartheta(\mu)Y(s)}{s^{jp}} - \frac{F(\mu, s)}{s^{jp}}\Big). \end{aligned} \tag{3.6}$$

Step 9. Under the assumption that $\lim_{s\to\infty}$, we compute Eq (3.6) to obtain:

$$\lim_{s\to\infty} s^{Kp+2}ARes_K(\mu,s) = \lim_{s\to\infty} s^{Kp+2}\Big(\frac{\hbar_0(\mu)}{s^2} + \frac{\hbar_1(\mu)}{s^{p+2}} + \cdots + \frac{\hbar_w(\mu)}{s^{wp+2}} + \sum_{r=w+1}^{K}\frac{\hbar_r(\mu)}{s^{rp+2}} - \sum_{j=0}^{q-1}\frac{D_\tau^j\omega(\mu,0)}{s^{jp+2}} + \frac{\vartheta(\mu)Y(s)}{s^{jp}} - \frac{F(\mu,s)}{s^{jp}}\Big).$$

Step 10. One may get the value of $\hbar_K(\mu)$ by figuring out the equation given

$$\lim_{s\to\infty}(s^{Kp+2}ARes_K(\mu,s)) = 0,$$

where $K = w+1, w+2, \cdots$

Step 11. To obtain the K-approximate solution of Eq (3.3), substitute the values of $\hbar_K(\mu)$ with a $\Psi(\mu,s)$ series that has been truncated.

Step 12. In order to get the K-approximate solution $\omega_K(\mu,\tau)$, solve $\Psi_K(\mu,s)$ using the AIT.

3.2. The algorithm of ATIM

Consider the general PDE of the space-time-fractional order

$$D_\tau^p\omega(\mu,\tau) = \Phi\Big(\omega(\mu,\tau), D_\mu^\tau\omega(\mu,\tau), D_\mu^{2\tau}\omega(\mu,\tau), D_\mu^{3\tau}\omega(\mu,\tau)\Big),\ 0 < p,\tau \le 1, \tag{3.7}$$

which is subjected to the initial condition (IC)

$$\omega^{(k)}(\mu,0) = h_k,\ k = 0,1,2,\cdots,m-1, \tag{3.8}$$

The function $\omega(\mu,\tau)$ is unknown, while $\Phi\Big(\omega(\mu,\tau), D_\mu^\tau\omega(\mu,\tau), D_\mu^{2\tau}\omega(\mu,\tau), D_\mu^{3\tau}\omega(\mu,\tau)\Big)$ may be a nonlinear operator or linear of $\omega(\mu,\tau), D_\mu^\tau\omega(\mu,\tau), D_\mu^{2\tau}\omega(\mu,\tau)$ and $D_\mu^{3\tau}\omega(\mu,\tau)$. The subsequent equation can be derived by performing the AT operation on both of the sides of Eq (3.7)

$$A[\omega(\mu,\tau)] = \frac{1}{s^p}\Big(\sum_{k=0}^{m-1}\frac{\omega^{(k)}(\mu,0)}{s^{2-p+k}} + A\Big[\Phi\Big(\omega(\mu,\tau), D_\mu^\tau\omega(\mu,\tau), D_\mu^{2\tau}\omega(\mu,\tau), D_\mu^{3\tau}\omega(\mu,\tau)\Big)\Big]\Big). \tag{3.9}$$

When the problem is resolved utilizing the AIT yields

$$\omega(\mu,\tau) = A^{-1}\Big[\frac{1}{s^p}\Big(\sum_{k=0}^{m-1}\frac{\omega^{(k)}(\mu,0)}{s^{2-p+k}} + A\Big[\Phi\Big(\omega(\mu,\tau), D_\mu^\tau\omega(\mu,\tau), D_\mu^{2\tau}\omega(\mu,\tau), D_\mu^{3\tau}\omega(\mu,\tau)\Big)\Big]\Big)\Big]. \tag{3.10}$$

The outcome of employing the ATIM is denoted by an infinite series

$$\omega(\mu,\tau) = \sum_{i=0}^{\infty}\omega_i. \tag{3.11}$$

Since $\Phi\Big(\omega, D_\mu^\tau\omega, D_\mu^{2\tau}\omega, D_\mu^{3\tau}\omega\Big)$ is either a nonlinear or linear operator, which can be decomposed as follows:

$$\begin{aligned}\Phi\Big(\omega, D_\mu^\tau\omega, D_\mu^{2\tau}\omega, D_\mu^{3\tau}\omega\Big) &= \Phi\Big(\omega_0, D_\mu^\tau\omega_0, D_\mu^{2\tau}\omega_0, D_\mu^{3\tau}\omega_0\Big)\\ &+ \sum_{i=0}^{\infty}\Bigg(\Phi\Big(\sum_{k=0}^{i}\Big(\omega_k, D_\mu^\tau\omega_k, D_\mu^{2\tau}\omega_k, D_\mu^{3\tau}\omega_k\Big)\Big) - \Phi\Big(\sum_{k=1}^{i-1}\Big(\omega_k, D_\mu^\tau\omega_k, D_\mu^{2\tau}\omega_k, D_\mu^{3\tau}\omega_k\Big)\Big)\Bigg).\end{aligned} \tag{3.12}$$

When the values of (3.11) and (3.12) are substituted for Eq (3.10), the subsequent equation is generated.

$$\begin{aligned}
&\sum_{i=0}^{\infty}\omega_i(\mu,\tau) = A^{-1}\Big[\frac{1}{s^p}\Big(\sum_{k=0}^{m-1}\frac{\omega^{(k)}(\mu,0)}{s^{2-p+k}} + A[\Phi(\omega_0, D_\mu^\tau\omega_0, D_\mu^{2\tau}\omega_0, D_\mu^{3\tau}\omega_0)]\Big)\Big]\\
&+ A^{-1}\Big[\frac{1}{s^p}\Big(A\Big[\sum_{i=0}^{\infty}\Big(\Phi\sum_{k=0}^{i}(\omega_k, D_\mu^\tau\omega_k, D_\mu^{2\tau}\omega_k, D_\mu^{3\tau}\omega_k)\Big)\Big]\Big)\Big] \qquad (3.13)\\
&- A^{-1}\Big[\frac{1}{s^p}\Big(A\Big[\Big(\Phi\sum_{k=1}^{i-1}(\omega_k, D_\mu^\tau\omega_k, D_\mu^{2\tau}\omega_k, D_\mu^{3\tau}\omega_k)\Big)\Big]\Big)\Big],
\end{aligned}$$

$$\begin{aligned}
&\omega_0(\mu,\tau) = A^{-1}\Big[\frac{1}{s^p}\Big(\sum_{k=0}^{m-1}\frac{\omega^{(k)}(\mu,0)}{s^{2-p+k}}\Big)\Big],\\
&\omega_1(\mu,\tau) = A^{-1}\Big[\frac{1}{s^p}\Big(A[\Phi(\omega_0, D_\mu^\tau\omega_0, D_\mu^{2\tau}\omega_0, D_\mu^{3\tau}\omega_0)]\Big)\Big],\\
&\vdots \qquad (3.14)\\
&\omega_{m+1}(\mu,\tau) = A^{-1}\Big[\frac{1}{s^p}\Big(A\Big[\sum_{i=0}^{\infty}\Big(\Phi\sum_{k=0}^{i}(\omega_k, D_\mu^\tau\omega_k, D_\mu^{2\tau}\omega_k, D_\mu^{3\tau}\omega_k)\Big)\Big]\Big)\Big]\\
&- A^{-1}\Big[\frac{1}{s^p}\Big(A\Big[\Big(\Phi\sum_{k=1}^{i-1}(\omega_k, D_\mu^\tau\omega_k, D_\mu^{2\tau}\omega_k, D_\mu^{3\tau}\omega_k)\Big)\Big]\Big)\Big],\ m = 1, 2, \cdots
\end{aligned}$$

For the analytical approximation of the solution to Eq (3.7)'s m-term, the subsequent expression may be employed

$$\omega(\mu,\tau) = \sum_{i=0}^{m-1}\omega_i. \qquad (3.15)$$

Example 3.1. *Consider the time-fractional diffusion model to investigate by ARPSM [32]:*

$$D_\tau^p\omega(\mu,\psi,\tau) - \frac{\partial^2\omega(\mu,\psi,\tau)}{\partial\mu^2} - \frac{\partial^2\omega(\mu,\psi,\tau)}{\partial\psi^2} = 0, \qquad (3.16)$$

which is subjected to the IC

$$\omega(\mu,\psi,0) = e^{\mu+\psi}. \qquad (3.17)$$

The exact solution to Example 3.1 for the integer case, i.e., for $p = 1$, reads

$$\omega(\mu,\psi,\tau) = e^{\mu+\psi+2\tau}. \qquad (3.18)$$

By applying AT to Eq (3.16) and with the help of Eq (3.17), we get

$$\omega(\mu,\psi,s) - \frac{e^{\mu+\psi}}{s^2} - \frac{1}{s^p}\Big[\frac{\partial^2\omega(\mu,\psi,s)}{\partial\mu^2}\Big] - \frac{1}{s^p}\Big[\frac{\partial^2\omega(\mu,\psi,s)}{\partial\psi^2}\Big] = 0. \qquad (3.19)$$

Thus, the term series that are required is generally given as

$$\omega(\mu,\psi,s)=\frac{e^{\mu+\psi}}{s^2}+\sum_{r=1}^{k}\frac{f_r(\mu,\psi,s)}{s^{rp+1}},\quad r=1,2,3,4,\cdots \tag{3.20}$$

The ARFs are given by

$$A_\tau Res(\mu,\psi,s)=\omega(\mu,\psi,s)-\frac{e^{\mu+\psi}}{s^2}-\frac{1}{s^p}\Big[\frac{\partial^2\omega(\mu,\psi,s)}{\partial\mu^2}\Big]-\frac{1}{s^p}\Big[\frac{\partial^2\omega(\mu,\psi,s)}{\partial\psi^2}\Big]=0, \tag{3.21}$$

and the k^{th}-LRFs as

$$A_\tau Res_k(\mu,\psi,s)=\omega_k(\mu,\psi,s)-\frac{e^{\mu+\psi}}{s^2}-\frac{1}{s^p}\Big[\frac{\partial^2\omega_k(\mu,\psi,s)}{\partial\mu^2}\Big]-\frac{1}{s^p}\Big[\frac{\partial^2\omega_k(\mu,\psi,s)}{\partial\psi^2}\Big]=0. \tag{3.22}$$

In finding $f_r(\mu,\psi,s)$, for $r=1,2,3,....$ We solve the expression $\lim_{s\to\infty}(s^{rp+1})$ by multiplying the final equation by s^{rp+1}, substituting the r^{th}-ARF Eq (3.22) for the r^{th}-truncated series Eq (3.20). $A_\tau Res_{\omega,r}(\mu,\psi,s))=0$, and $r=1,2,3,\cdots$. Following are its few terms:

$$f_1(\mu,\psi,s)=2e^{\mu+\psi}, \tag{3.23}$$

$$f_2(\mu,\psi,s)=4e^{\mu+\psi}, \tag{3.24}$$

$$f_3(\mu,\psi,s)=8e^{\mu+\psi}, \tag{3.25}$$

and so on.
Putting the values of $f_r(\mu,s)$, $r=1,2,3,\cdots$, in Eq (3.20), we get

$$\omega(\mu,\psi,s)=\frac{e^{\mu+\psi}}{s^2}+\frac{2e^{\mu+\psi}}{s^{p+1}}+\frac{4e^{\mu+\psi}}{s^{2p+1}}+\frac{8e^{\mu+\psi}}{s^{3p+1}}+\cdots \tag{3.26}$$

AIT is applied to get

$$\omega(\mu,\psi,\tau)=e^{\mu+\psi}\Big(1+\frac{2\tau^p}{\Gamma(p+1)}+\frac{4\tau^{2p}}{\Gamma(2p+1)}+\frac{8\tau^{3p}}{\Gamma(3p+1)}+\cdots\Big). \tag{3.27}$$

Now, we proceed to apply ATIM for analyzing Example 3.1. The result obtained by applying the AT on both sides of Eq (3.16) reads

$$A[D_\tau^p\omega(\mu,\psi,\tau)]=\frac{1}{s^p}\Big(\sum_{k=0}^{m-1}\frac{\omega^{(k)}(\mu,\psi,0)}{s^{2-p+k}}+A\Big[\frac{\partial^2\omega(\mu,\psi,\tau)}{\partial\mu^2}+\frac{\partial^2\omega(\mu,\psi,\tau)}{\partial\psi^2}\Big]\Big). \tag{3.28}$$

The result obtained by applying the AIT on both sides of Eq (3.28) reads

$$\omega(\mu,\psi,\tau)=A^{-1}\Big[\frac{1}{s^p}\Big(\sum_{k=0}^{m-1}\frac{\omega^{(k)}(\mu,\psi,0)}{s^{2-p+k}}+A\Big[\frac{\partial^2\omega(\mu,\psi,\tau)}{\partial\mu^2}+\frac{\partial^2\omega(\mu,\psi,\tau)}{\partial\psi^2}\Big]\Big)\Big]. \tag{3.29}$$

By iteratively applying the AT, the following equation is obtained:

$$\omega_0(\mu,\psi,\tau) = A^{-1}\Big[\frac{1}{s^p}\Big(\sum_{k=0}^{m-1}\frac{\omega^{(k)}(\mu,\psi,0)}{s^{2-p+k}}\Big)\Big] = A^{-1}\Big[\frac{\omega(\mu,\psi,0)}{s^2}\Big] = e^{\mu+\psi}.$$

The equivalent form was obtained by substituting the RL integral into Eq (3.16)

$$\omega(\mu,\psi,\tau) = e^{\mu+\psi} - A\Big[\frac{\partial^2\omega(\mu,\psi,\tau)}{\partial\mu^2} + \frac{\partial^2\omega(\mu,\psi,\tau)}{\partial\psi^2}\Big]. \tag{3.30}$$

The subsequent terms are attainable through the utilization of the ATIM procedure:

$$\begin{aligned}
\omega_0(\mu,\psi,\tau) &= e^{\mu+\psi},\\
\omega_1(\mu,\psi,\tau) &= \frac{2\tau^p e^{\mu+\psi}}{\Gamma(p+1)},\\
\omega_2(\mu,\psi,\tau) &= \frac{4\tau^{2p} e^{\mu+\psi}}{\Gamma(2p+1)},\\
\omega_3(\mu,\psi,\tau) &= \frac{8\tau^{3p} e^{\mu+\psi}}{\Gamma(3p+1)}.
\end{aligned} \tag{3.31}$$

The following constitutes the final solution of the ATIM procedure:

$$\omega(\mu,\psi,\tau) = \omega_0(\mu,\psi,\tau) + \omega_1(\mu,\psi,\tau) + \omega_2(\mu,\psi,\tau) + \omega_3(\mu,\psi,\tau) + \cdots \tag{3.32}$$

$$\omega(\mu,\psi,\tau) = e^{\mu+\psi}\Big(1 + \frac{2\tau^p}{\Gamma(p+1)} + \frac{4\tau^{2p}}{\Gamma(2p+1)} + \frac{8\tau^{3p}}{\Gamma(3p+1)} + \cdots\Big). \tag{3.33}$$

The approximation (3.27) using ARPSM has the same form as the approximation (3.33) using ATIM. Since these approximations are entirely symmetrical, we will analyze only one of them in the numerical analysis. The numerical and graphical analysis of the approximations (3.27)/(3.33) is demonstrated in Figures 1 and 2 and Table 1. Figure 1 examines the impact of the fractional parameter p on the wave behavior as defined by the approximations (3.27)/(3.33). It is observed that the behavior of these waves is greatly influenced by the fractional parameter p, as demonstrated in Figure 1. This is one of the most important goals of studying the behavior of non-linear phenomena described by fractional differential equations, because their solutions reveal the ambiguity about these phenomena' behavior and properties that non-fractal differential equations cannot. Also, we assessed the accuracy and stability of the approximations (3.27)/(3.33) by comparing them with the exact solution (3.18) for the integer case. This verification is evident in Figure 2. Furthermore, we conducted a numerical analysis of these approximations and estimated the absolute error compared to the exact solution for the integer case, as depicted in Table 1. Table 1 helps to obtain a deeper and more precise understanding of the analysis results of the test function wave solutions computed by two different solution methods. This table quantitatively compares several values of p and analyzes how these methods are efficient in solving the test Example 3.1.

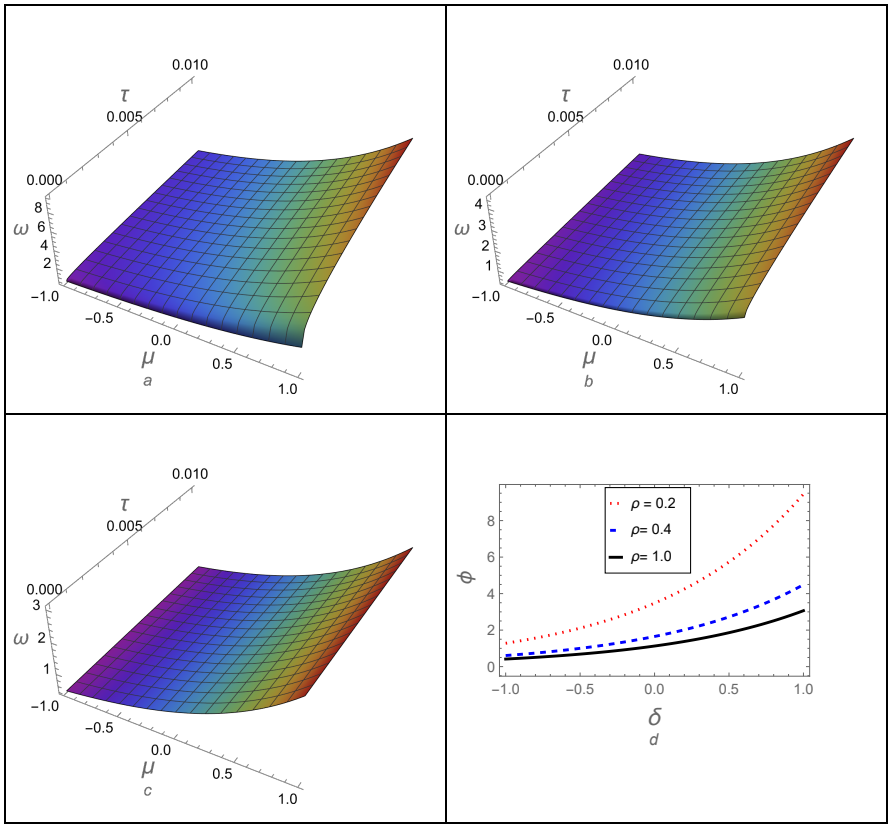

Figure 1. The approximations (3.27)/(3.33) using ARPSM/ATIM are plotted against p: (a) $p = 0.2$ for $\psi = 0.1$, (b) $p = 0.4$ for $\psi = 0.1$, (c) $p = 1$ for $\psi = 0.1$, (d) the comparison between (a), (b), and (c) for $\tau = 0.1$ and $\psi = 0.1$.

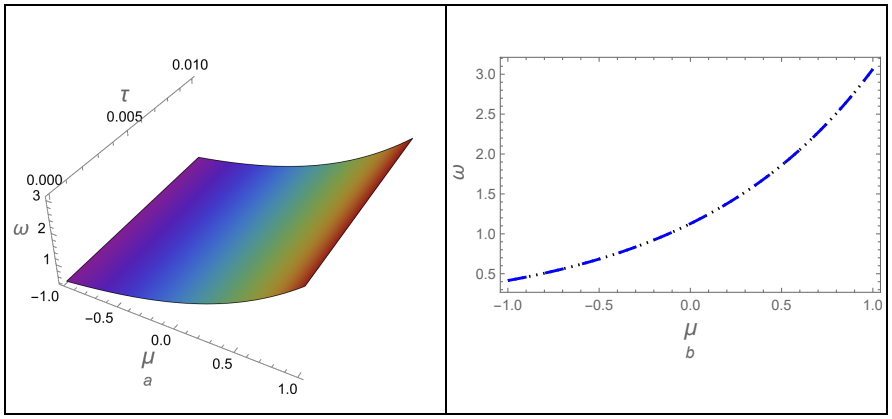

Figure 2. A comparison between the approximations (3.27)/(3.33) using ARPSM/ATIM and the exact solution (3.18) for the integer case: (a) three-dimensional graphic at $\psi = 0.1$ and (b) two-dimensional graphic at $\tau = 0.1$ and $\psi = 0.1$.

Table 1. Analyzing the obtained approximations (3.27)/(3.33) of Example 3.1 using ARPSM/ATIM against p for $\tau = 0.01$ and $\psi = 0.1$.

μ	$ARPSM/ATIM$ p=0.5	$ARPSM/ATIM$ p=0.7	$ARPSM/ATIM$ p=1.0	$Exact$	$Error_{p=1.0}$
0.0	1.39879	1.20765	1.12750	1.12750	1.480958×10^{-6}
0.2	1.70848	1.47503	1.37713	1.37713	1.808846×10^{-6}
0.4	2.08675	1.80161	1.68203	1.68203	2.209330×10^{-6}
0.6	2.54876	2.20049	2.05443	2.05443	2.698482×10^{-6}
0.8	3.11306	2.68768	2.50929	2.50929	3.295933×10^{-6}
1.0	3.80230	3.28274	3.06485	3.06485	4.025662×10^{-6}
1.2	4.64414	4.00955	3.74342	3.74342	4.916955×10^{-6}
1.4	5.67237	4.89728	4.57222	4.57223	6.005583×10^{-6}
1.6	6.92824	5.98155	5.58452	5.58453	7.335235×10^{-6}
1.8	8.46218	7.30588	6.82095	6.82096	8.959277×10^{-6}
2.0	10.3357	8.92343	8.33113	8.33114	1.094290×10^{-5}

Example 3.2. *Consider the time-fractional heat model to investigate by ARPSM [34]:*

$$D_{\tau}^{p}\omega(\mu,\psi,\tau) - \frac{\partial^2\omega(\mu,\psi,\tau)}{\partial\mu^2} - \frac{\partial^2\omega(\mu,\psi,\tau)}{\partial\psi^2} = 0, \tag{3.34}$$

which is subjected to the IC

$$\omega(\mu,\psi,0) = \sin(\mu)\cos(\psi). \tag{3.35}$$

The exact solution to Example 3.2 for the integer case, i.e., for $p = 1$, reads

$$\omega(\mu,\psi,\tau) = e^{-2\tau}\sin(\mu)\cos(\psi). \tag{3.36}$$

The result obtained by applying the AT on both sides of Eq (3.35) reads

$$\omega(\mu,\psi,s) - \frac{\sin(\mu)\cos(\psi)}{s^2} - \frac{1}{s^p}\Big[\frac{\partial^2\omega(\mu,\psi,s)}{\partial\mu^2}\Big] - \frac{1}{s^p}\Big[\frac{\partial^2\omega(\mu,\psi,s)}{\partial\psi^2}\Big] = 0. \tag{3.37}$$

Thus, the term series that are required is generally given as

$$\omega(\mu,\psi,s) = \frac{\sin(\mu)\cos(\psi)}{s^2} + \sum_{r=1}^{k}\frac{f_r(\mu,\psi,s)}{s^{rp+1}}, \quad r = 1,2,3,4,\cdots \tag{3.38}$$

The following is ARFs:

$$A_{\tau}Res(\mu,\psi,s) = \omega(\mu,\psi,s) - \frac{\sin(\mu)\cos(\psi)}{s^2} - \frac{1}{s^p}\Big[\frac{\partial^2\omega(\mu,\psi,s)}{\partial\mu^2}\Big] - \frac{1}{s^p}\Big[\frac{\partial^2\omega(\mu,\psi,s)}{\partial\psi^2}\Big] = 0, \tag{3.39}$$

and the k^{th}-LRFs as

$$A_{\tau}Res_k(\mu,\psi,s) = \omega_k(\mu,\psi,s) - \frac{\sin(\mu)\cos(\psi)}{s^2} - \frac{1}{s^p}\Big[\frac{\partial^2\omega_k(\mu,\psi,s)}{\partial\mu^2}\Big] - \frac{1}{s^p}\Big[\frac{\partial^2\omega_k(\mu,\psi,s)}{\partial\psi^2}\Big] = 0. \tag{3.40}$$

In finding $f_r(\mu,\psi,s)$, for $r = 1,2,3,....$ We solve the expression $\lim_{s\to\infty}(s^{rp+1})$ by multiplying the final equation by s^{rp+1}, substituting the r^{th}-ARF Eq (3.40) for the r^{th}-truncated series Eq (3.38). $A_\tau Res_{\omega,r}(\mu,\psi,s)) = 0$, and $r = 1,2,3,\cdots$. Following are its few terms:

$$f_1(\mu,\psi,s) = -2\sin(\mu)\cos(\psi), \tag{3.41}$$

$$f_2(\mu,\psi,s) = 4\sin(\mu)\cos(\psi), \tag{3.42}$$

$$f_3(\mu,\psi,s) = -8\sin(\mu)\cos(\psi), \tag{3.43}$$

and so on.

Putting the values of $f_r(\mu,s)$, $r = 1,2,3,\cdots$, in Eq (3.38), we deduce

$$\omega(\mu,\psi,s) = \frac{\sin(\mu)\cos(\psi)}{s^2} - \frac{2\sin(\mu)\cos(\psi)}{s^{p+1}} + \frac{4\sin(\mu)\cos(\psi)}{s^{2p+1}} - \frac{8\sin(\mu)\cos(\psi)}{s^{3p+1}} + \cdots \tag{3.44}$$

The following constitutes the final solution of the ARPSM procedure:

$$\omega(\mu,\psi,\tau) = \omega_0(\mu,\psi,\tau) + \omega_1(\mu,\psi,\tau) + \omega_2(\mu,\psi,\tau) + \omega_3(\mu,\psi,\tau) + \cdots \tag{3.45}$$

$$\omega(\mu,\psi,\tau) = \sin(\mu)\cos(\psi)\Big(1 - \frac{2\tau^p}{\Gamma(p+1)} + \frac{4\tau^{2p}}{\Gamma(2p+1)} - \frac{8\tau^{3p}}{\Gamma(3p+1)} + \cdots\Big). \tag{3.46}$$

Now, we proceed to apply ATIM for analyzing Example 3.2. The result obtained by applying the AT on both sides of Eq (3.34) reads

$$A[D_\tau^p\omega(\mu,\psi,\tau)] = \frac{1}{s^p}\Big(\sum_{k=0}^{m-1}\frac{\omega^{(k)}(\mu,\psi,0)}{s^{2-p+k}} + A\Big[\frac{\partial^2\omega(\mu,\psi,\tau)}{\partial\mu^2} + \frac{\partial^2\omega(\mu,\psi,\tau)}{\partial\psi^2}\Big]\Big). \tag{3.47}$$

The result obtained by applying the AIT on both sides of Eq (3.47) is as follows:

$$\omega(\mu,\psi,\tau) = A^{-1}\Big[\frac{1}{s^p}\Big(\sum_{k=0}^{m-1}\frac{\omega^{(k)}(\mu,\psi,0)}{s^{2-p+k}} + A\Big[\frac{\partial^2\omega(\mu,\psi,\tau)}{\partial\mu^2} + \frac{\partial^2\omega(\mu,\psi,\tau)}{\partial\psi^2}\Big]\Big)\Big]. \tag{3.48}$$

By iteratively applying the AT, the following equation is obtained:

$$\omega_0(\mu,\psi,\tau) = A^{-1}\Big[\frac{1}{s^p}\Big(\sum_{k=0}^{m-1}\frac{\omega^{(k)}(\mu,\psi,0)}{s^{2-p+k}}\Big)\Big] = A^{-1}\Big[\frac{\omega(\mu,\psi,0)}{s^2}\Big] = \sin(\mu)\cos(\psi).$$

The equivalent form was obtained by substituting the RL integral into Eq (3.34)

$$\omega(\mu,\psi,\tau) = \sin(\mu)\cos(\psi) - A\Big[\frac{\partial^2\omega(\mu,\psi,\tau)}{\partial\mu^2} + \frac{\partial^2\omega(\mu,\psi,\tau)}{\partial\psi^2}\Big]. \tag{3.49}$$

The subsequent terms are attainable through the utilization of the ATIM procedure:

$$\begin{aligned}
\omega_0(\mu,\psi,\tau) &= \sin(\mu)\cos(\psi),\\
\omega_1(\mu,\psi,\tau) &= -\frac{2\tau^p\sin(\mu)\cos(\psi)}{\Gamma(p+1)},\\
\omega_2(\mu,\psi,\tau) &= \frac{4\tau^{2p}\sin(\mu)\cos(\psi)}{\Gamma(2p+1)},\\
\omega_3(\mu,\psi,\tau) &= -\frac{8\tau^{2p}\sin(\mu)\cos(\psi)}{\Gamma(2p+1)}.
\end{aligned} \tag{3.50}$$

The following constitutes the final solution of the ATIM procedure:

$$\omega(\mu,\psi,\tau) = \omega_0(\mu,\psi,\tau) + \omega_1(\mu,\psi,\tau) + \omega_2(\mu,\psi,\tau) + \omega_3(\mu,\psi,\tau) + \cdots \tag{3.51}$$

$$\omega(\mu,\psi,\tau) = \sin(\mu)\cos(\psi)\Big(1 - \frac{2\tau^p}{\Gamma(p+1)} + \frac{4\tau^{2p}}{\Gamma(2p+1)} - \frac{8\tau^{3p}}{\Gamma(3p+1)} + \cdots\Big). \tag{3.52}$$

It is clear from the approximation (3.46) that using ARPSM is the same approximation (3.52) using ATIM. Since these approximations are completely symmetrical, we will analyze only one of them in the numerical analysis. Figures 3 and 4 and Table 2 exhibit the numerical and graphical examination of the approximations (3.46)/(3.52). Figure 3 examines the influence of the fractional parameter p on the profile of approximations (3.46)/(3.52). It is shown that the behavior of these waves is significantly impacted by changing the value of the fractional parameter p. Moreover, the approximations (3.46)/(3.52) are compared to the exact solution (3.36) in order to confirm their high level of accuracy, as shown in Figure 4. Additionally, we performed a quantitative study of these approximations and calculated the absolute error compared to the exact solution (3.36) for the integer case, as illustrated in Table 2. This table facilitates a more comprehensive and accurate comprehension of the analysis findings from the test function wave solutions computed using two distinct solution approaches. This Table provides a quantitative comparison of several values of p and examines the efficiency of different strategies for the test problem. Additionally, we performed a quantitative study of these approximations and calculated the absolute error compared to the exact solution (3.36) for the integer case, as illustrated in Table 2. This Table provides a quantitative comparison of several values of p and examines the efficiency of the used approaches for the current test Example 3.2.

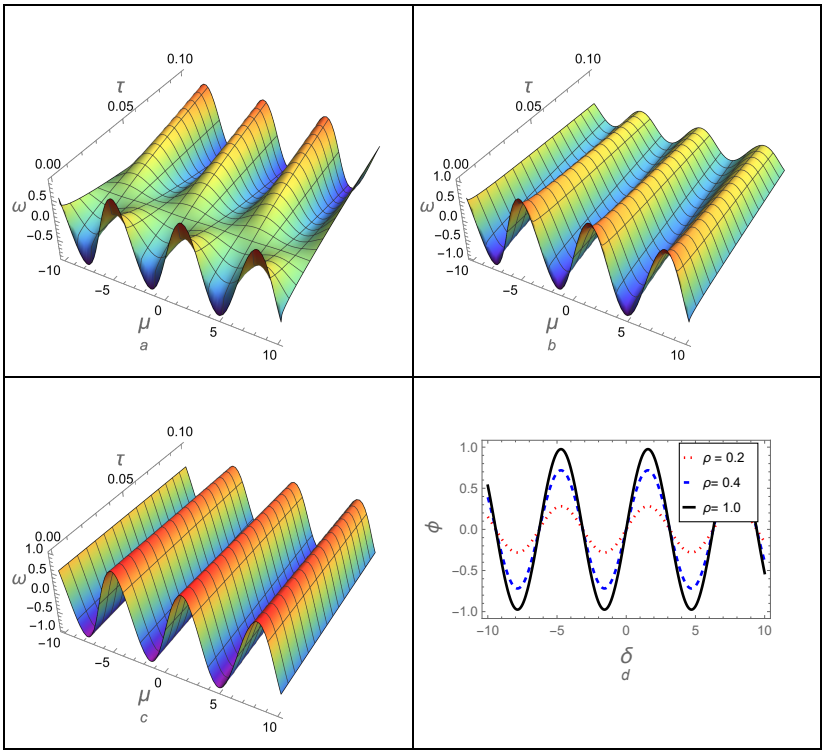

Figure 3. The approximations (3.46)/(3.52) using ARPSM/ATIM are plotted against p: (a) $p = 0.2$ for $\psi = 0.1$, (b) $p = 0.4$ for $\psi = 0.1$, (c) $p = 1$ for $\psi = 0.1$, (d) the comparison between (a), (b), and (c) for $\tau = 0.1$ and $\psi = 0.1$.

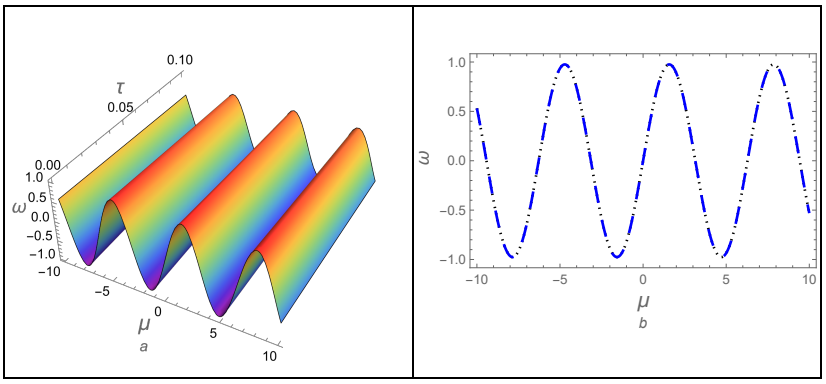

Figure 4. A comparison between the approximations (3.46)/(3.52) using ARPSM/ATIM and the exact solution (3.36) for the integer case: (a) three-dimensional graphic at $\psi = 0.1$ and (b) two-dimensional graphic at $\tau = 0.1$ and $\psi = 0.1$.

Table 2. Analyzing the obtained approximations (3.46)/(3.52) of Example 3.2 using ARPSM/ATIM against p for $\tau = 0.1$ and $\psi = 0.1$.

μ	$ARPSM/ATIM$ p=0.5	$ARPSM/ATIM$ p=0.7	$ARPSM/ATIM$ p=1.0	$Exact$	$Error_{p=1.0}$
0.2	0.098056	0.130488	0.161831	0.161844	1.26684×10^{-5}
0.4	0.192204	0.255773	0.317211	0.317236	2.48317×10^{-5}
0.6	0.278688	0.370861	0.459945	0.459981	3.60051×10^{-5}
0.8	0.354062	0.471165	0.584342	0.584387	4.57431×10^{-5}
1.0	0.415321	0.552684	0.685443	0.685496	5.36574×10^{-5}
1.2	0.460022	0.612170	0.759217	0.759277	5.94326×10^{-5}
1.4	0.486384	0.647251	0.802724	0.802787	6.28384×10^{-5}
1.6	0.493355	0.656527	0.814229	0.814293	6.37391×10^{-5}
1.8	0.480658	0.639630	0.793274	0.793336	6.20986×10^{-5}
2.0	0.448798	0.597233	0.740693	0.740751	5.79825×10^{-5}

Example 3.3. *Consider the time-fractional Burger's model to investigate by ARPSM [44]:*

$$D_\tau^p \omega(\mu,\psi,\tau) - \frac{\partial^2\omega(\mu,\psi,\tau)}{\partial\mu} - \frac{\partial^2\omega(\mu,\psi,\tau)}{\partial\psi} - \omega(\mu,\psi,\tau)\frac{\partial\omega(\mu,\psi,\tau)}{\partial\mu} = 0, \tag{3.53}$$

which is subjected to the IC:

$$\omega(\mu,\psi,0) = \mu + \psi. \tag{3.54}$$

The exact solution to Example 3.3 for the integer case, i.e., for $p = 1$, reads

$$\omega(\mu,\psi,\tau) = \frac{\mu+\psi}{1-\tau}. \tag{3.55}$$

The result obtained by applying the AT on both sides of Eq (3.54) reads

$$\begin{aligned}\omega(\mu,\psi,s) - \frac{\mu+\psi}{s^p} - \frac{1}{s^p}\Big[\frac{\partial^2\omega(\mu,\psi,s)}{\partial\mu}\Big] - \frac{1}{s^p}\Big[\frac{\partial^2\omega(\mu,\psi,s)}{\partial\psi}\Big] \\ - \frac{1}{s^p}A_\tau\Big[A_\tau^{-1}\omega(\mu,\psi,s) \times \frac{\partial A_\tau^{-1}\omega(\mu,\psi,s)}{\partial\mu}\Big] = 0.\end{aligned} \tag{3.56}$$

Thus, the term series that are required is generally given as

$$\omega(\mu,\psi,s)=\frac{\mu+\psi}{s^2}+\sum_{r=1}^{k}\frac{f_r(\mu,\psi,s)}{s^{rp+1}},\quad r=1,2,3,4\cdots \tag{3.57}$$

The ARFs are given by

$$\begin{aligned}A_\tau Res(\mu,\psi,s)=\omega(\mu,\psi,s)-\frac{\mu+\psi}{s^p}-\frac{1}{s^p}\Big[\frac{\partial^2\omega(\mu,\psi,s)}{\partial\mu}\Big]-\frac{1}{s^p}\Big[\frac{\partial^2\omega(\mu,\psi,s)}{\partial\psi}\Big]\\-\frac{1}{s^p}A_\tau\Big[A_\tau^{-1}\omega(\mu,\psi,s)\times\frac{\partial A_\tau^{-1}\omega(\mu,\psi,s)}{\partial\mu}\Big]=0,\end{aligned} \tag{3.58}$$

and the k^{th}-LRFs as

$$\begin{aligned}A_\tau Res_k(\mu,\psi,s)=\omega_k(\mu,\psi,s)-\frac{\mu+\psi}{s^p}-\frac{1}{s^p}\Big[\frac{\partial^2\omega_k(\mu,\psi,s)}{\partial\mu}\Big]-\frac{1}{s^p}\Big[\frac{\partial^2\omega_k(\mu,\psi,s)}{\partial\psi}\Big]\\-\frac{1}{s^p}A_\tau\Big[A_\tau^{-1}\omega_k(\mu,\psi,s)\times\frac{\partial A_\tau^{-1}\omega_k(\mu,\psi,s)}{\partial\mu}\Big]=0.\end{aligned} \tag{3.59}$$

In finding $f_r(\mu,\psi,s)$, for $r=1,2,3,....$ We solve the expression $\lim_{s\to\infty}(s^{rp+1})$ by multiplying the final equation by s^{rp+1}, substituting the r^{th}-ARF Eq (3.59) for the r^{th}-truncated series Eq (3.57). $A_\tau Res_{\omega,r}(\mu,\psi,s))=0$, and $r=1,2,3,\cdots$. Following are its few terms:

$$f_1(\mu,\psi,s)=\mu+\psi, \tag{3.60}$$

$$f_2(\mu,\psi,s)=2(\mu+\psi), \tag{3.61}$$

$$f_3(\mu,\psi,s)=4(\mu+\psi). \tag{3.62}$$

and so on.
Putting the values of $f_r(\mu,s)$, $r=1,2,3,\cdots$, in Eq (3.57), we deduce

$$\omega(\mu,\psi,s)=\frac{\mu+\psi}{s^2}+\frac{\mu+\psi}{s^{p+1}}+\frac{2(\mu+\psi)}{s^{2p+1}}+\frac{4(\mu+\psi)}{s^{3p+1}}+\cdots \tag{3.63}$$

AIT is applied to get

$$\omega(\mu,\psi,\tau)=(\mu+\psi)\Big(1+\frac{\tau^p}{\Gamma(p+1)}+\frac{2\tau^{2p}}{\Gamma(2p+1)}+\frac{4\tau^{3p}}{\Gamma(3p+1)}+\cdots\Big). \tag{3.64}$$

Now, we proceed to apply ATIM for analyzing Example 3.3. The result obtained by applying the AT on both sides of Eq (3.53) reads

$$\begin{aligned}&A[D_\tau^p\omega(\mu,\psi,\tau)]\\&=\frac{1}{s^p}\Big(\sum_{k=0}^{m-1}\frac{\omega^{(k)}(\mu,\psi,0)}{s^{2-p+k}}+A\Big[\frac{\partial^2\omega(\mu,\psi,\tau)}{\partial\mu}+\frac{\partial^2\omega(\mu,\psi,\tau)}{\partial\psi}+\omega(\mu,\psi,\tau)\frac{\partial\omega(\mu,\psi,\tau)}{\partial\mu}\Big]\Big).\end{aligned} \tag{3.65}$$

The result obtained by applying the AIT on both sides of (3.65) *reads*

$$\omega(\mu,\psi,\tau)=A^{-1}\Big[\frac{1}{s^p}\Big(\sum_{k=0}^{m-1}\frac{\omega^{(k)}(\mu,\psi,0)}{s^{2-p+k}}+A\Big[\frac{\partial^2\omega(\mu,\psi,\tau)}{\partial\mu}+\frac{\partial^2\omega(\mu,\psi,\tau)}{\partial\psi}+\omega(\mu,\psi,\tau)\frac{\partial\omega(\mu,\psi,\tau)}{\partial\mu}\Big]\Big)\Big]. \quad (3.66)$$

By applying the AT to the above equation, we get

$$\omega_0(\mu,\psi,\tau)=A^{-1}\Big[\frac{1}{s^p}\Big(\sum_{k=0}^{m-1}\frac{\omega^{(k)}(\mu,\psi,0)}{s^{2-p+k}}\Big)\Big]=A^{-1}\Big[\frac{\omega(\mu,\psi,0)}{s^2}\Big]=\mu+\psi.$$

The equivalent form was obtained by substituting the RL integral into Eq (3.53)

$$\omega(\mu,\psi,\tau)=\mu+\psi-A\Big[\frac{\partial^2\omega(\mu,\psi,\tau)}{\partial\mu}+\frac{\partial^2\omega(\mu,\psi,\tau)}{\partial\psi}+\omega(\mu,\psi,\tau)\frac{\partial\omega(\mu,\psi,\tau)}{\partial\mu}\Big]. \quad (3.67)$$

The subsequent terms are attainable through the utilization of the ATIM procedure:

$$\begin{aligned}
&\omega_0(\mu,\psi,\tau)=\mu+\psi,\\
&\omega_1(\mu,\psi,\tau)=\frac{\tau^p(\mu+\psi)}{\Gamma(p+1)},\\
&\omega_2(\mu,\psi,\tau)=\frac{\tau^{2p}(\mu+\psi)\left(\frac{\tau^p\Gamma(2p+1)^2}{\Gamma(p+1)^2\Gamma(3p+1)}+2\right)}{\Gamma(2p+1)},\\
&\omega_3(\mu,\psi,\tau)=\Big(\tau^{4p}(\mu+\psi)\Big(\Big(\sqrt{\pi}4^{1-3p}\tau^{2p}\Gamma(p+1)^2\Gamma(2p+1)^2\Gamma(5p+1)\Big)/\Big(\Gamma\Big(3p+\frac{1}{2}\Big)\Big)\\
&+\Big(\tau^{3p}\Gamma(2p+1)^4\Gamma(6p+1)\Big)/\Big(\Gamma(7p+1)\Big)+\Big(2\tau^p\Gamma(p+1)\Gamma(3p+1)\Big(2\Gamma(3p+1)\Gamma(p+1)^3\\
&+\Gamma(2p+1)^3\Big)\Gamma(4p+1)\Big)/\Big(\Gamma(5p+1)\Big)+\Big(\sqrt{\pi}4^{1-2p}\Gamma(p+1)^3\Gamma(3p+1)^3\Big)/\Big(\Gamma\Big(2p+\frac{1}{2}\Big)\Big)\Big)\Big)/\Big(\Gamma(p\\
&+1)^4\Gamma(2p+1)^2\Gamma(3p+1)^2\Big).
\end{aligned} \quad (3.68)$$

The following constitutes the final solution using the ATIM procedure:

$$\omega(\mu,\psi,\tau)=\omega_0(\mu,\psi,\tau)+\omega_1(\mu,\psi,\tau)+\omega_2(\mu,\psi,\tau)+\omega_3(\mu,\psi,\tau)+\cdots \quad (3.69)$$

$$\begin{aligned}
\omega(\mu,\psi,\tau)&=\mu+\psi+\frac{\tau^p(\mu+\psi)}{\Gamma(p+1)}+\frac{\tau^{2p}(\mu+\psi)\left(\frac{\tau^p\Gamma(2p+1)^2}{\Gamma(p+1)^2\Gamma(3p+1)}+2\right)}{\Gamma(2p+1)}\\
&+\Big(\tau^{4p}(\mu+\psi)\Big(\Big(\sqrt{\pi}4^{1-3p}\tau^{2p}\Gamma(p+1)^2\Gamma(2p+1)^2\Gamma(5p+1)\Big)/\Big(\Gamma\Big(3p+\frac{1}{2}\Big)\Big)\\
&+\Big(\tau^{3p}\Gamma(2p+1)^4\Gamma(6p+1)\Big)/\Big(\Gamma(7p+1)\Big)+\Big(2\tau^p\Gamma(p+1)\Gamma(3p+1)\Big(2\Gamma(3p+1)\Gamma(p+1)^3\\
&+\Gamma(2p+1)^3\Big)\Gamma(4p+1)\Big)/\Big(\Gamma(5p+1)\Big)+\Big(\sqrt{\pi}4^{1-2p}\Gamma(p+1)^3\Gamma(3p+1)^3\Big)/\Big(\Gamma\Big(2p+\frac{1}{2}\Big)\Big)\Big)\Big)/\Big(\Gamma(p\\
&+1)^4\Gamma(2p+1)^2\Gamma(3p+1)^2\Big)+\cdots
\end{aligned} \quad (3.70)$$

Figure 5 demonstrates the impact of the fractional parameter on the behavior of the approximation (3.64) using ARPSM of Example 3.3. Figure 6 presents a visual comparison between

the approximation (3.64) using ARPSM and the exact solution (3.55) for the integer case. In addition, we investigated the approximation (3.70) using ATIM, which is illustrated in Figures 7 and 8. The approximations (3.64)/(3.70) and the exact solution (3.55) for the integer case show complete agreement (see Figures 6 and 8), which enhances the strength, accuracy, and efficiency of these methods in analyzing more complicated evolution equations. By comparing and analyzing Figures 5–8, we can evaluate the performance of the ARPSM/ATIM method in solving Burger's model's constraints. Tables 3 and 4 provide a detailed analysis of different p values for the approximations (3.64) and (3.70) using ARPSM and ATIM, respectively. In addition, Table 5 compares the absolute error for the two approximations (3.64) and (3.70) as compared to the exact solution (3.55).

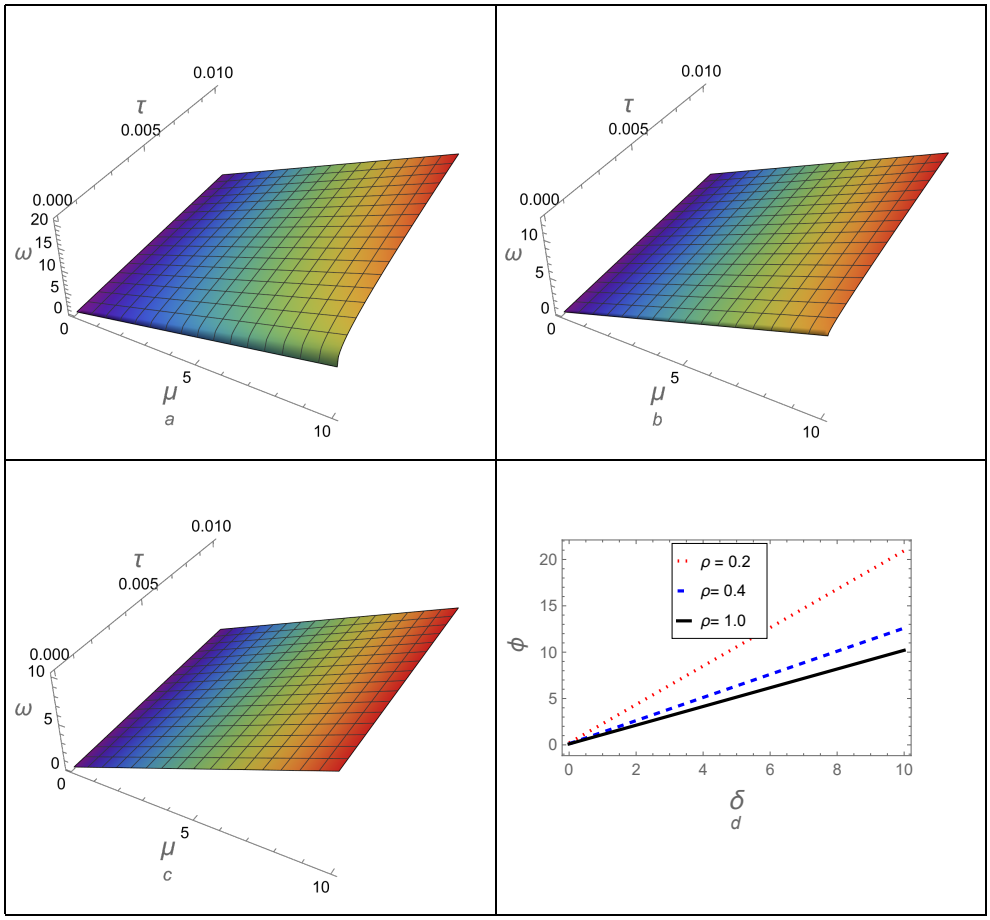

Figure 5. The approximation (3.64) using ARPSM is plotted against p: (a) $p = 0.2$ for $\psi = 0.1$, (b) $p = 0.4$ for $\psi = 0.1$, (c) $p = 1$ for $\psi = 0.1$, (d) the comparison between (a), (b), and (c) for $\tau = 0.1$ and $\psi = 0.1$.

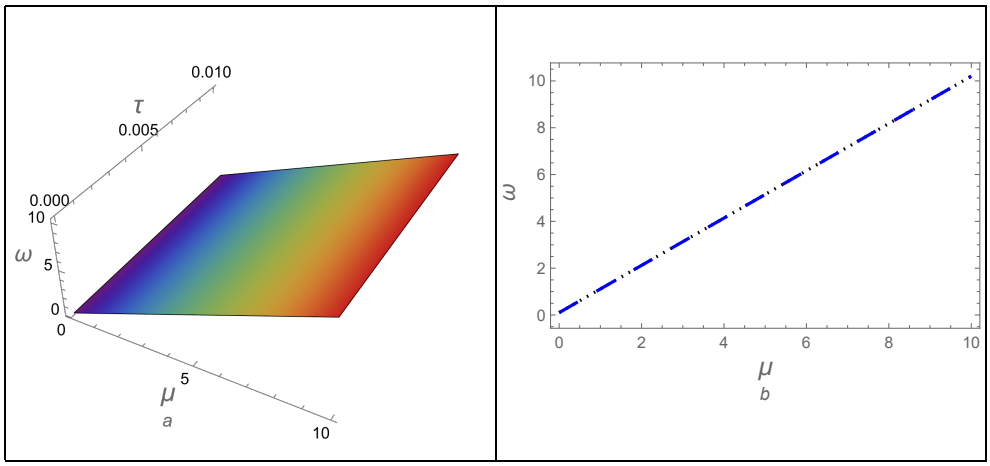

Figure 6. A comparison between the approximation (3.64) using ARPSM and the exact solution (3.55) for the integer case: (a) three-dimensional graphic at $\psi = 0.1$ and (b) two-dimensional graphic at $\tau = 0.1$ and $\psi = 0.1$.

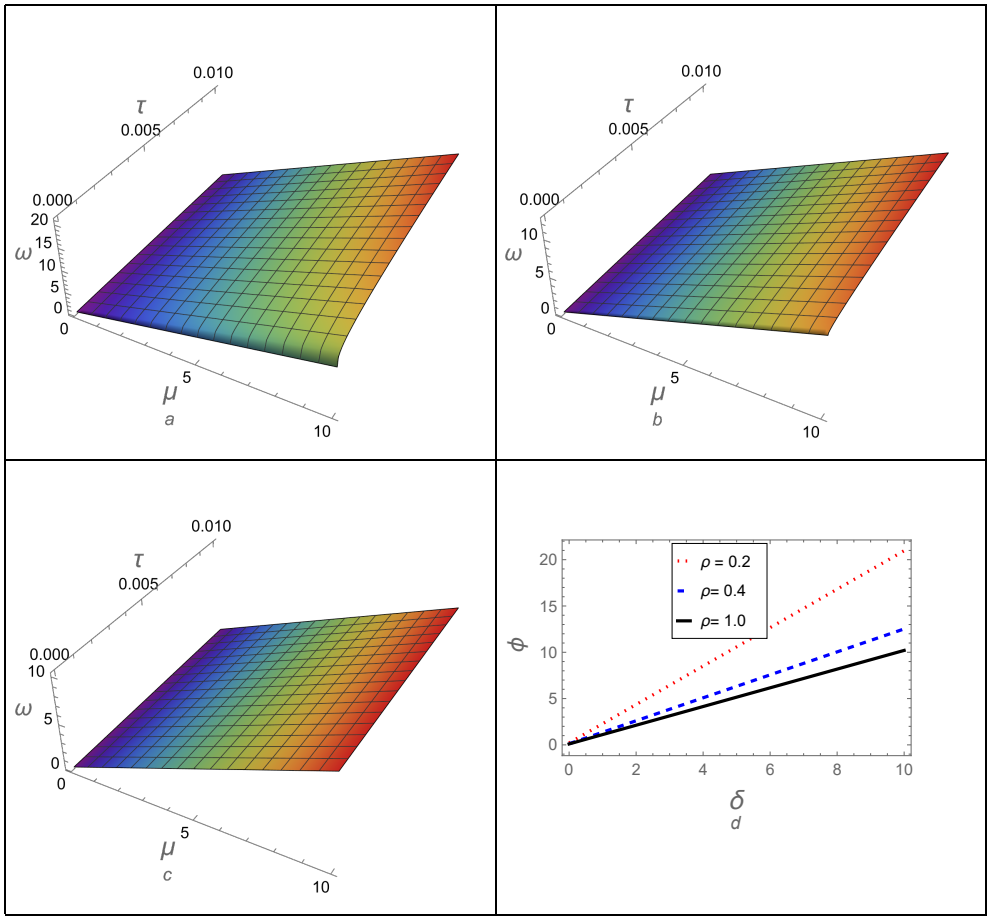

Figure 7. The approximation (3.70) using ATIM is plotted against p: (a) $p = 0.2$ for $\psi = 0.1$, (b) $p = 0.4$ for $\psi = 0.1$, (c) $p = 1$ for $\psi = 0.1$, (d) the comparison between (a), (b), and (c) for $\tau = 0.1$ and $\psi = 0.1$.

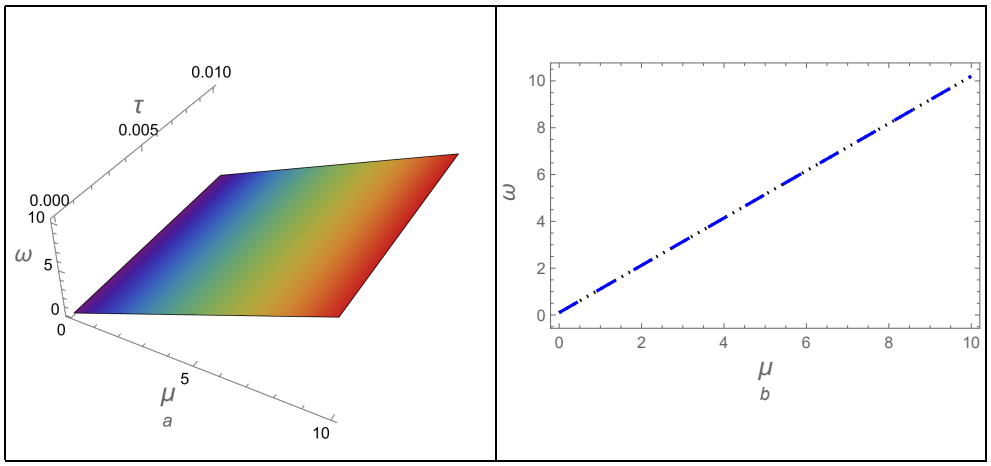

Figure 8. A comparison between the approximation (3.70) using ARPSM and the exact solution (3.55)) for the integer case: (a) three-dimensional graphic at $\psi = 0.1$ and (b) two-dimensional graphic at $\tau = 0.1$ and $\psi = 0.1$.

Table 3. Analyzing the approximation (3.64) using ARPSM against p for $\tau = 0.1$.

μ	$ARPSM_{p=0.5}$	$ARPSM_{p=0.7}$	$ARPSM_{p=1.0}$	$Exact$	$Error_{p=1.0}$
0.0	0.113585	0.104648	0.101010	0.101010	3.434343×10^{-8}
0.2	0.340754	0.313944	0.303030	0.303030	1.030303×10^{-7}
0.4	0.567923	0.523240	0.505050	0.505050	1.717171×10^{-7}
0.6	0.795093	0.732536	0.707070	0.707070	2.404040×10^{-7}
0.8	1.022260	0.941832	0.909090	0.909090	3.090909×10^{-7}
1.0	1.249430	1.151130	1.111111	1.111111	3.777777×10^{-7}
1.2	1.476600	1.360420	1.313130	1.313130	4.464646×10^{-7}
1.4	1.703770	1.569720	1.515150	1.515150	5.151515×10^{-7}
1.6	1.930940	1.779020	1.717170	1.717170	5.838383×10^{-7}
1.8	2.158110	1.988310	1.919190	1.919190	6.525252×10^{-7}
2.0	2.385280	2.197610	2.121210	2.121210	7.212121×10^{-7}

Table 4. Analyzing the approximation (3.70) using ATIM against p for $\tau = 0.01$ and $\psi = 0.1$.

μ	$ATIM_{p=0.5}$	$ATIM_{p=0.7}$	$ATIM_{p=1.0}$	$Exact$	$Error_{p=1.0}$
0.0	0.113413	0.104641	0.10101	0.101010	6.717342×10^{-8}
0.2	0.340240	0.313924	0.30303	0.303030	2.015202×10^{-7}
0.4	0.567067	0.523206	0.50505	0.505051	3.358671×10^{-7}
0.6	0.793894	0.732489	0.70707	0.707071	4.702139×10^{-7}
0.8	1.020720	0.941772	0.90909	0.909091	6.045608×10^{-7}
1.0	1.247550	1.151050	1.11111	1.111110	7.389076×10^{-7}
1.2	1.474380	1.360340	1.31313	1.313130	8.732545×10^{-7}
1.4	1.701200	1.569620	1.51515	1.515150	1.007601×10^{-6}
1.6	1.928030	1.778900	1.71717	1.717170	1.141948×10^{-6}
1.8	2.154860	1.988180	1.91919	1.919190	1.276295×10^{-6}
2.0	2.381680	2.197470	2.12121	2.121210	1.410641×10^{-6}

Table 5. A comparison between the absolute errors of the two approximations (3.64) and (3.70).

μ	$ARPSM_{p=1}$	$ATIM_{p=1}$	$Exact$	$Error_{ARPSM}$	$Error_{ATIM}$
0.0	0.10101	0.10101	0.10101	3.434343×10^{-8}	6.717342×10^{-8}
0.2	0.30303	0.30303	0.30303	1.030303×10^{-7}	2.015202×10^{-7}
0.4	0.50505	0.50505	0.50505	1.717171×10^{-7}	3.358671×10^{-7}
0.6	0.70707	0.70707	0.70707	2.404040×10^{-7}	4.702139×10^{-7}
0.8	0.90909	0.90909	0.90909	3.090909×10^{-7}	6.045608×10^{-7}
1.0	1.11111	1.11111	1.11111	3.777777×10^{-7}	7.389076×10^{-7}
1.2	1.31313	1.31313	1.31313	4.464646×10^{-7}	8.732545×10^{-7}
1.4	1.51515	1.51515	1.51515	5.151515×10^{-7}	1.007601×10^{-6}
1.6	1.71717	1.71717	1.71717	5.838383×10^{-7}	1.141948×10^{-6}
1.8	1.91919	1.91919	1.91919	6.525252×10^{-7}	1.276295×10^{-6}
2.0	2.12121	2.12121	2.12121	7.212121×10^{-7}	1.410641×10^{-6}

4. Conclusions

Our study has provided new insights into the dynamics of some physical time-fractional differential equations, including heat, diffusion, and Burger equations. Both the Aboodh residual power series approach and the Aboodh transform iterative method have been applied to investigate time-fractional equations inside the Caputo operator framework. These approaches have proven to be efficient and accurate tools for solving fractional equations and offering insights into the behavior and characteristics of fractional systems. By employing these methods, we have not only captured the non-local and memory-dependent characteristics inherent to time-fractional dynamics but also paved the way for potential applications in understanding and predicting the complex behavior of these systems. The obtained outcomes highlight the importance of fractional calculus in modeling different nonlinear phenomena associated with various physical and engineering systems and solving more complicated differential equations related to other natural applications. The analytical approximations of the Aboodh techniques facilitate future studies and applications in several scientific and engineering fields, including physics, biology, finance, and many others. In summary, our study advances the field of fractional calculus by offering novel approaches for analyzing time-fractional equations. This enriches our understanding of the underlying dynamics and opens new avenues for future investigations and practical implementations.

5. Future work

Given the favorable outcomes achieved via the Aboodh techniques, we can employ these techniques to examine various evolutionary equations that can be utilized to depict many nonlinear structures (waves) that emerge and propagate in diverse plasma systems and various physical systems. For instance, the fluid equations for various plasma models can be reduced to different fractional evolution (wave) equations. These equations are employed to model and describe the properties of different nonlinear structures, such as solitary waves, shock waves, and cnoidal waves that propagate in diverse plasma systems, including KdV-type equations [69, 70], Kawahara-type equations [71, 72] Burgers-

type equations [73]. On the other hand, using one of the reductive perturbation methods, the fluid equations for many different plasma models can also be reduced to the nonlinear Schodinger-type equations [74, 75], which are used to describe many modulated envelope structures that propagate at group velocity, such as dark-, bright-, gray-solitons, rogue waves and breathers, and modulated cnoidal waves. Therefore, Aboodh's methods can be applied to analyze these equations.

Authors contributions

All authors contributed equally and approved the final version of the current manuscript.

Use of AI tools declaration

The authors declare they have not used Artificial Intelligence (AI) tools in the creation of this article.

Acknowledgments

The authors express their gratitude to Princess Nourah bint Abdulrahman University Researchers Supporting Project number (PNURSP2024R2), Princess Nourah bint Abdulrahman University, Riyadh, Saudi Arabia. This work was supported by the Deanship of Scientific Research, Vice Presidency for Graduate Studies and Scientific Research, King Faisal University, Saudi Arabia (GrantA263).

Conflict of interest

The authors declare that they have no conflicts of interest.

Funding

The authors express their gratitude to Princess Nourah bint Abdulrahman University Researchers Supporting Project number (PNURSP2024R2), Princess Nourah bint Abdulrahman University, Riyadh, Saudi Arabia. This work was supported by the Deanship of Scientific Research, Vice Presidency for Graduate Studies and Scientific Research, King Faisal University, Saudi Arabia (GrantA263).

References

1. H. Srivastava, R. Shah, H. Khan, M. Arif, Some analytical and numerical investigation of a family of fractional-order Helmholtz equations in two space dimensions, *Math. Method. Appl. Sci.*, **43** (2020), 199–212. http://dx.doi.org/10.1002/mma.5846
2. A. Alshehry, M. Imran, A. Khan, R. Shah, W. Weera, Fractional view analysis of Kuramoto-Sivashinsky equations with non-singular kernel operators, *Symmetry*, **14** (2022), 1463. http://dx.doi.org/10.3390/sym14071463

3. H. Yasmin, N. Aljahdaly, A. Saeed, R. Shah, Investigating symmetric soliton solutions for the fractional coupled konno-onno system using improved versions of a novel analytical technique, *Mathematics*, **11** (2023), 2686. http://dx.doi.org/10.3390/math11122686
4. S. El-Tantawy, H. Alyousef, R. Matoog, R. Shah, On the optical soliton solutions to the fractional complex structured (1+1)-dimensional perturbed gerdjikov-ivanov equation, *Phys. Scr.*, **99** (2024), 035249. http://dx.doi.org/10.1088/1402-4896/ad241b
5. S. El-Tantawy, R. Matoog, A. Alrowaily, S. Ismaeel, On the shock wave approximation to fractional generalized Burger-Fisher equations using the residual power series transform method, *Phys. Fluids*, **36** (2024), 023105. http://dx.doi.org/10.1063/5.0187127
6. J. Machado, V. Kiryakova, F. Mainardi, Recent history of fractional calculus, *Commun. Nonlinear Sci.*, **16** (2011), 1140–1153. http://dx.doi.org/10.1016/j.cnsns.2010.05.027
7. J. Liu, F. Geng, An explanation on four new definitions of fractional operators, *Acta Math. Sci.*, **44** (2024), 1271–1279. http://dx.doi.org/10.1007/s10473-024-0405-7
8. A. Majeed, M. Kamran, M. Iqbal, D. Baleanu, Solving time fractional Burgers and Fishers equations using cubic B-spline approximation method, *Adv. Differ. Equ.*, **2020** (2020), 175. http://dx.doi.org/10.1186/s13662-020-02619-8
9. D. Li, C. Wu, Z. Zhang, Linearized Galerkin FEMs for nonlinear time fractional parabolic problems with non-smooth solutions in time direction, *J. Sci. Comput.*, **80** (2019), 403–419. http://dx.doi.org/10.1007/s10915-019-00943-0
10. M. Hajad, V. Tangwarodomnukun, C. Jaturanonda, C. Dumkum, Laser cutting path optimization using simulated annealing with an adaptive large neighborhood search, *Int. J. Adv. Manuf. Technol.*, **103** (2019), 781–792. http://dx.doi.org/10.1007/s00170-019-03569-6
11. R. El-Nabulsi, The fractional Boltzmann transport equation, *Comput. Math. Appl.*, **62** (2011), 1568–1575. http://dx.doi.org/10.1016/j.camwa.2011.03.040
12. A. Khan, J. Iqbal, R. Shah, A new efficient two-step iterative method for solving absolute value equations, *Eng. Computation.*, **41** (2024), 597–610. http://dx.doi.org/10.1108/EC-11-2023-0781
13. A. Atangana, J. Gomez-Aguilar, Numerical approximation of Riemann Liouville definition of fractional derivative: from Riemann-Liouville to Atangana-Baleanu, *Numer. Meth. Part. D. E.*, **34** (2018), 1502–1523. http://dx.doi.org/10.1002/num.22195
14. D. Baleanu, S. Etemad, S. Rezapour, A hybrid Caputo fractional modeling for thermostat with hybrid boundary value conditions, *Bound. Value Probl.*, **2020** (2020), 64. http://dx.doi.org/10.1186/s13661-020-01361-0
15. H. Mohammadi, S. Kumar, S. Rezapour, S. Etemad, A theoretical study of the Caputo-Fabrizio fractional modeling for hearing loss due to Mumps virus with optimal control, *Chaos Soliton. Fract.*, **144** (2021), 110668. http://dx.doi.org/10.1016/j.chaos.2021.110668
16. L. He, A. Valocchi, C. Duarte, A transient global-local generalized FEM for parabolic and hyperbolic PDEs with multi-space/time scales, *J. Comput. Phys.*, **488** (2023), 112179. http://dx.doi.org/10.1016/j.jcp.2023.112179
17. L. He, A. Valocchi, C. Duarte, An adaptive global-local generalized FEM for multiscale advection-diffusion problems, *Comput. Method. Appl. M.*, **418** (2024), 116548. http://dx.doi.org/10.1016/j.cma.2023.116548

18. Y. Kai, S. Chen, K. Zhang, Z. Yin, Exact solutions and dynamic properties of a nonlinear fourth-order time-fractional partial differential equation, *Waves Random Complex*, in press. http://dx.doi.org/10.1080/17455030.2022.2044541
19. Y. Kai, J. Ji, Z. Yin, Study of the generalization of regularized long-wave equation, *Nonlinear Dyn.*, **107** (2022), 2745–2752. http://dx.doi.org/10.1007/s11071-021-07115-6
20. W. Liu, X. Bai, H. Yang, R. Bao, J. Liu, Tendon driven bistable origami flexible gripper for high-speed adaptive grasping, *IEEE Robot. Autom. Let.*, **9** (2024), 5417–5424. http://dx.doi.org/10.1109/LRA.2024.3389413
21. B. Cuahutenango-Barro, M. Taneco-Hernandez, J. Gomez-Aguilar, On the solutions of fractional-time wave equation with memory effect involving operators with regular kernel, *Chaos Soliton. Fract.*, **115** (2018), 283–299. http://dx.doi.org/10.1016/j.chaos.2018.09.002
22. J. Gomez-Gardenes, V. Latora, Entropy rate of diffusion processes on complex networks, *Phys. Rev. E*, **78** (2008), 065102. http://dx.doi.org/10.1103/PhysRevE.78.065102
23. A. Lopes, J. Tenreiro Machado, Entropy analysis of soccer dynamics, *Entropy*, **21** (2019), 187. http://dx.doi.org/10.3390/e21020187
24. A. Bejan, Second-law analysis in heat transfer and thermal design, *Advances in Heat Transfer*, **15** (1982), 1–58. http://dx.doi.org/10.1016/S0065-2717(08)70172-2
25. M. Syam, M. Al-Refai, Solving fractional diffusion equation via the collocation method based on fractional Legendre functions, *Journal of Computational Methods in Physics*, **2014** (2014), 381074. http://dx.doi.org/10.1155/2014/381074
26. E. Lenzi, M. Dos Santos, F. Michels, R. Mendes, L. Evangelista, Solutions of some nonlinear diffusion equations and generalized entropy framework, *Entropy*, **15** (2013), 3931–3940. http://dx.doi.org/10.3390/e15093931
27. J. Prehl, F. Boldt, K. Hoffmann, C. Essex, Symmetric fractional diffusion and entropy production, *Entropy*, **18** (2016), 275. http://dx.doi.org/10.3390/e18070275
28. M. Dehghan, M. Abbaszadeh, A finite difference/finite element technique with error estimate for space fractional tempered diffusion-wave equation, *Comput. Math. Appl.*, **75** (2018), 2903–2914. http://dx.doi.org/10.1016/j.camwa.2018.01.020
29. S. Lei, Y. Huang, Fast algorithms for high-order numerical methods for space-fractional diffusion equations, *Int. J. Comput. Math.*, **94** (2017), 1062–1078. http://dx.doi.org/10.1080/00207160.2016.1149579
30. N. Tripathi, S. Das, S. Ong, H. Jafari, M. Al Qurashi, Solution of higher order nonlinear time-fractional reaction diffusion equation, *Entropy*, **18** (2016), 329. http://dx.doi.org/10.3390/e18090329
31. D. Kumar, J. Singh, S. Kumar, Numerical computation of fractional multi-dimensional diffusion equations by using a modified homotopy perturbation method, *Journal of the Association of Arab Universities for Basic and Applied Sciences*, **17** (2015), 20–26. http://dx.doi.org/10.1016/j.jaubas.2014.02.002
32. F. Zafarghandi, M. Mohammadi, E. Babolian, S. Javadi, Radial basis functions method for solving the fractional diffusion equations, *Appl. Math. Comput.*, **342** (2019), 224–246. http://dx.doi.org/10.1016/j.amc.2018.08.043

33. A. Bejan, Second law analysis in heat transfer, *Energy*, **5** (1980), 720–732. http://dx.doi.org/10.1016/0360-5442(80)90091-2
34. S. Sarwar, S. Alkhalaf, S. Iqbal, M. Zahid, A note on optimal homotopy asymptotic method for the solutions of fractional order heat-and wave-like partial differential equations, *Comput. Math. Appl.*, **70** (2015), 942–953. http://dx.doi.org/10.1016/j.camwa.2015.06.017
35. A. Bokhari, G. Mohammad, M. Mustafa, F. Zaman, Adomian decomposition method for a nonlinear heat equation with temperature dependent thermal properties, *Math. Probl. Eng.*, **2009** (2009), 926086. http://dx.doi.org/10.1155/2009/926086
36. D. Shou, J. He, Beyond Adomian method: the variational iteration method for solving heat-like and wave-like equations with variable coefficients, *Phys. Lett. A*, **372** (2008), 233–237. http://dx.doi.org/10.1016/j.physleta.2007.07.011
37. D. Rostamy, K. Karimi, Bernstein polynomials for solving fractional heat- and wave-like equations, *FCAA*, **15** (2012), 556–571. http://dx.doi.org/10.2478/s13540-012-0039-7
38. C. Liu, S. Kong, S. Yuan, Reconstructive schemes for variational iteration method within Yang-Laplace transform with application to fractal heat conduction problem, *Therm. Sci.*, **17** (2013), 715–721. http://dx.doi.org/10.2298/TSCI120826075L
39. R. Nuruddeen, A. Nass, Exact solutions of wave-type equations by the Aboodh decomposition method, *Stochastic Modelling and Applications*, **21** (2017), 23–30.
40. R. Mittal, P. Singhal, Numerical solution of Burger's equation, *Commun. Numer. Meth. Eng.*, **9** (1993), 397–406. http://dx.doi.org/10.1002/cnm.1640090505
41. A. Esen, O. Tasbozan, Numerical solution of time fractional Burgers equation by cubic B-spline finite elements, *Mediterr. J. Math.*, **13** (2016), 1325–1337. http://dx.doi.org/10.1007/s00009-015-0555-x
42. A. Esen, N. Yagmurlu, O. Tasbozan, Approximate analytical solution to time-fractional damped Burger and Cahn-Allen equations, *Appl. Math. Inf. Sci.*, **7** (2013), 1951–1956. http://dx.doi.org/10.12785/amis/070533
43. E. Abdel-Salam, E. Yousif, Y. Arko, E. Gumma, Solution of moving boundary space-time fractional Burger's equation, *J. Appl. Math.*, **2014** (2014), 218092. http://dx.doi.org/10.1155/2014/218092
44. M. Inc, The approximate and exact solutions of the space-and time-fractional Burgers equations with initial conditions by variational iteration method, *J. Math. Anal. Appl.*, **345** (2008), 476–484. http://dx.doi.org/10.1016/j.jmaa.2008.04.007
45. O. Arqub, Series solution of fuzzy differential equations under strongly generalized differentiability, *J. Adv. Res. Appl. Math.*, **5** (2013), 31–52. http://dx.doi.org/10.5373/jaram.1447.051912
46. O. Arqub, Z. Abo-Hammour, R. Al-Badarneh, S. Momani, A reliable analytical method for solving higher-order initial value problems, *Discrete Dyn. Nat. Soc.*, **2013** (2013), 673829. http://dx.doi.org/10.1155/2013/673829
47. O. Arqub, A. El-Ajou, Z. Zhour, S. Momani, Multiple solutions of nonlinear boundary value problems of fractional order: a new analytic iterative technique, *Entropy*, **16** (2014), 471–493. http://dx.doi.org/10.3390/e16010471

48. A. El-Ajou, O. Arqub, S. Momani, Approximate analytical solution of the nonlinear fractional KdV-Burgers equation: a new iterative algorithm, *J. Comput. Phys.*, **293** (2015), 81–95. http://dx.doi.org/10.1016/j.jcp.2014.08.004

49. F. Xu, Y. Gao, X. Yang, H. Zhang, Construction of fractional power series solutions to fractional Boussinesq equations using residual power series method, *Math. Probl. Eng.*, **2016** (2016), 5492535. http://dx.doi.org/10.1155/2016/5492535

50. J. Zhang, Z. Wei, L. Li, C. Zhou, Least-squares residual power series method for the time-fractional differential equations, *Complexity*, **2019** (2019), 6159024. http://dx.doi.org/10.1155/2019/6159024

51. I. Jaradat, M. Alquran, R. Abdel-Muhsen, An analytical framework of 2D diffusion, wave-like, telegraph, and Burgers' models with twofold Caputo derivatives ordering, *Nonlinear Dyn.*, **93** (2018), 1911–1922. http://dx.doi.org/10.1007/s11071-018-4297-8

52. I. Jaradat, M. Alquran, K. Al-Khaled, An analytical study of physical models with inherited temporal and spatial memory, *Eur. Phys. J. Plus*, **133** (2018), 162. http://dx.doi.org/10.1140/epjp/i2018-12007-1

53. M. Liaqat, A. Khan, M. Alam, M. Pandit, S. Etemad, S. Rezapour, Approximate and closed-form solutions of Newell-Whitehead-Segel equations via modified conformable Shehu transform decomposition method, *Math. Probl. Eng.*, **2022** (2022), 6752455. http://dx.doi.org/10.1155/2022/6752455

54. M. Alquran, M. Ali, M. Alsukhour, I. Jaradat, Promoted residual power series technique with Laplace transform to solve some time-fractional problems arising in physics, *Results Phys.*, **19** (2020), 103667. http://dx.doi.org/10.1016/j.rinp.2020.103667

55. T. Eriqat, A. El-Ajou, M. Oqielat, Z. Al-Zhour, S. Momani, A new attractive analytic approach for solutions of linear and nonlinear neutral fractional pantograph equations, *Chaos Soliton. Fract.*, **138** (2020), 109957. http://dx.doi.org/10.1016/j.chaos.2020.109957

56. M. Alquran, M. Alsukhour, M. Ali, I. Jaradat, Combination of Laplace transform and residual power series techniques to solve autonomous n-dimensional fractional nonlinear systems, *Nonlinear Engineering*, **10** (2021), 282–292. http://dx.doi.org/10.1515/nleng-2021-0022

57. A. Khan, M. Junaid, I. Khan, F. Ali, K. Shah, D. Khan, Application of homotopy analysis natural transform method to the solution of nonlinear partial differential equations, *Sci. Int. (Lahore)*, **29** (2017), 297–303.

58. M. Zhang, Y. Liu, X. Zhou, Efficient homotopy perturbation method for fractional non-linear equations using Sumudu transform, *Therm. Sci.*, **19** (2015), 1167–1171. http://dx.doi.org/10.2298/TSCI1504167Z

59. G. Ojo, N. Mahmudov, Aboodh transform iterative method for spatial diffusion of a biological population with fractional-order, *Mathematics*, **9** (2021), 155. http://dx.doi.org/10.3390/math9020155

60. M. Awuya, D. Subasi, Aboodh transform iterative method for solving fractional partial differential equation with Mittag-Leffler Kernel, *Symmetry*, **13** (2021), 2055. http://dx.doi.org/10.3390/sym13112055

61. A. Ganie, S. Noor, M. Al Huwayz, A. Shafee, S. El-Tantawy, Numerical simulations for fractional Hirota-Satsuma coupled Korteweg-de Vries systems, *Open Phys.*, **22** (2024), 20240008. http://dx.doi.org/10.1515/phys-2024-0008
62. S. Noor, W. Albalawi, R. Shah, M. Al-Sawalha, S. Ismaeel, S. El-Tantawy, On the approximations to fractional nonlinear damped Burgers-type equations that arise in fluids and plasmas using Aboodh residual power series and Aboodh transform iteration methods, *Front. Phys.*, **12** (2024), 1374481. http://dx.doi.org/10.3389/fphy.2024.1374481
63. S. Noor, W. Albalawi, R. Shah, A. Shafee, S. Ismaeel, S. El-Tantawy, A comparative analytical investigation for some linear and nonlinear time-fractional partial differential equations in the framework of the Aboodh transformation, *Front. Phys.*, **12** (2024), 1374049. http://dx.doi.org/10.3389/fphy.2024.1374049
64. K. Aboodh, The new integral transform "Aboodh transform", *Global Journal of Pure and Applied Mathematics*, **9** (2013), 35–43.
65. S. Aggarwal, R. Chauhan, A comparative study of Mohand and Aboodh transforms, *International Journal of Research in Advent Technology*, **7** (2019), 520–529.
66. M. Benattia, K. Belghaba, Application of the Aboodh transform for solving fractional delay differential equations, *Universal Journal of Mathematics and Applications*, **3** (2020), 93–101. http://dx.doi.org/10.32323/ujma.702033
67. B. Delgado, J. Macias-Diaz, On the general solutions of some non-homogeneous div-curl systems with Riemann-Liouville and Caputo fractional derivatives, *Fractal Fract.*, **5** (2021), 117. http://dx.doi.org/10.3390/fractalfract5030117
68. S. Alshammari, M. Al-Smadi, I. Hashim, M. Alias, Residual power series technique for simulating fractional Bagley-Torvik problems emerging in applied physics, *Appl. Sci.*, **9** (2019), 5029. http://dx.doi.org/10.3390/app9235029
69. W. Albalawi, S. El-Tantawy, S. Alkhateeb, The phase shift analysis of the colliding dissipative KdV solitons, *J. Ocean Eng. Sci.*, **7** (2022), 521–527. http://dx.doi.org/10.1016/j.joes.2021.09.021
70. B. Kashkari, S. El-Tantawy, A. Salas, L. El-Sherif, Homotopy perturbation method for studying dissipative nonplanar solitons in an electronegative complex plasma, *Chaos Soliton. Fract.*, **130** (2020), 109457. http://dx.doi.org/10.1016/j.chaos.2019.109457
71. H. Alyousef, A. Salas, R. Matoog, S. El-Tantawy, On the analytical and numerical approximations to the forced damped Gardner Kawahara equation and modeling the nonlinear structures in a collisional plasma, *Phys. Fluids*, **34** (2022), 103105. http://dx.doi.org/10.1063/5.0109427
72. S. El-Tantawy, A. Salas, H. Alyouse, M. Alharthi, Novel exact and approximate solutions to the family of the forced damped Kawahara equation and modeling strong nonlinear waves in a plasma, *Chinese J. Phys.*, **77** (2022), 2454–2471. http://dx.doi.org/10.1016/j.cjph.2022.04.009
73. A. Wazwaz, W. Alhejaili, S. El-Tantawy, Physical multiple shock solutions to the integrability of linear structures of Burgers hierarchy, *Phys. Fluids*, **35** (2023), 123101. http://dx.doi.org/10.1063/5.0177366
74. S. El-Tantawy, A. Salas, H. Alyousef, M. Alharthi, Novel approximations to a nonplanar nonlinear Schrodinger equation and modeling nonplanar rogue waves/breathers in a complex plasma, *Chaos Soliton. Fract.*, **163** (2022), 112612. http://dx.doi.org/10.1016/j.chaos.2022.112612

75. W. Alhejaili, B. Mouhammadoul, Alim, C. Tiofack, A. Mohamadou, S. El-Tantawy, Modulational instability and associated breathers in collisional electronegative non-Maxwellian plasmas, *Phys. Fluids*, **35** (2023), 103101. http://dx.doi.org/10.1063/5.0166059

AIMS Press